

1 **Carbon uptake and water use in woodlands and forests in southern**
2 **Australia during an extreme heat wave event in the ‘Angry**
3 **Summer’ of 2012/2013.**

4 Eva van Gorsel¹, Sebastian Wolf², James Cleverly³, Peter Isaac¹, Vanessa Haverd¹, Cécilia Ewenz⁴,
5 Stefan Arndt⁵, Jason Beringer⁶, Víctor Resco de Dios⁷, Bradley J. Evans⁸, Anne Griebel^{5,9}, Lindsay B.
6 Hutley¹⁰, Trevor Keenan¹¹, Natascha Kljun¹², Craig Macfarlane¹³, Wayne S. Meyer¹⁴, Ian McHugh¹⁵,
7 Elise Pendall⁹, Suzanne M. Prober¹³, Richard Silberstein¹⁶

8 1 CSIRO, Oceans and Atmosphere, Yarralumla, 2600, Australia

9 2 Department of Environmental Systems Science, ETH Zurich, 8092 Zurich, Switzerland

10 3 School of Life Sciences, University of Technology Sydney, Broadway, NSW, 2007, Australia

11 4 Airborne Research Australia, Flinders University, Salisbury South, SA, 5106, Australia

12 5 School of Ecosystem and Forest Sciences, The University of Melbourne, Richmond, 3121, Victoria, Australia

13 6 School of Earth and Environment (SEE), The University of Western Australia, Crawley, WA, 6009, Australia

14 7 Producció Vegetal i Ciència Forestal – Agrotecnio Centre, Universitat de Lleida, 25198, Lleida, Spain

15 8 School of Life and Environmental Sciences, The University of Sydney, Sydney, 2015, Australia

16 9 Hawkesbury Institute for the Environment, Western Sydney University, Penrith, NSW 2570

17 10 School of Environment, Research Institute for the Environment and Livelihoods, Charles Darwin University, NT,
18 Australia

19 11 Lawrence Berkeley National Lab., 1 Cyclotron Road, Berkeley CA, USA

20 12 Dept of Geography, College of Science, Swansea University, Singleton Park, Swansea, UK

21 13 CSIRO Land and Water, Private Bag 5, Floreat 6913, Western Australia

22 14 Environment Institute, The University of Adelaide, Adelaide SA 5 005, Australia

23 15 School of Earth, Atmosphere and Environment, Monash University, Clayton, 3800, Australia

24 16 Centre for Ecosystem Management, Edith Cowan University, School of Natural Sciences, Joondalup, WA, 6027,
25 Australia

26 *Correspondence to:* E. van Gorsel (eva.vangorsel@gmail.com)

27 **Abstract.** As a result of climate change warmer temperatures are projected through the 21st century and are already
28 increasing above modelled predictions. Apart from increases in the mean, warm/hot temperature extremes are expected to
29 become more prevalent in the future, along with an increase in the frequency of droughts. It is crucial to better understand

30 the response of terrestrial ecosystems to such temperature extremes for predicting land-surface feedbacks in a changing
31 climate. While land-surface feedbacks in drought conditions and during heat waves have been reported from Europe and
32 the US, direct observations of the impact of such extremes on the carbon and water cycles in Australia have been lacking.
33 During the 2012/2013 summer, Australia experienced a record-breaking heat wave with an exceptional spatial extent that
34 lasted for several weeks. In this study we synthesised eddy-covariance measurements from seven woodlands and one
35 forest site across three biogeographic regions in southern Australia. These observations were combined with model results
36 from BIOS2 (Haverd et al., 2013, *Biogeosciences*, 10: 2011-2040) to investigate the effect of the summer heat wave on
37 the carbon and water exchange of terrestrial ecosystems which are known for their resilience toward hot and dry
38 conditions. We found that water-limited woodland and energy-limited forest ecosystems responded differently to the heat
39 wave. During the most intense part of the heat wave, the woodlands experienced decreased latent heat flux (23% of
40 background value), increased Bowen ratio (154%) and reduced carbon uptake (60%). At the same time the forest
41 ecosystem showed increased latent heat flux (151%), reduced Bowen ratio (19%) and increased carbon uptake (112%).
42 Higher temperatures caused increased ecosystem respiration at all sites (up to 139%). During daytime all ecosystems
43 remained carbon sinks, but carbon uptake was reduced in magnitude. The number of hours during which the ecosystem
44 acted as a carbon sink was also reduced, which switched the woodlands into a carbon source on a daily average.
45 Precipitation occurred after the first, most intense part of the heat wave, and the subsequent cooler temperatures in the
46 temperate woodlands led to recovery of the carbon sink, decreased the Bowen ratio (65%) and hence increased
47 evaporative cooling. Gross primary productivity in the woodlands recovered quickly with precipitation and cooler
48 temperatures but respiration remained high. While the forest proved relatively resilient to this short-term heat extreme the
49 response of the woodlands is the first direct evidence that the carbon sinks of large areas of Australia may not be
50 sustainable in a future climate with an increased number, intensity and duration of heat waves.

51 **1 Introduction**

52 Average temperatures in Australia have increased by 0.9°C since 1910 (CSIRO and BOM, 2014), which represents the
53 most extreme of modeling scenarios, and even further warming is projected with climate change (IPCC, 2013). In addition
54 to increased mean temperature, warm temperature extremes are becoming more frequent in Australia and worldwide
55 (Lewis and King, 2015, Steffen, 2015) and an increased prevalence of drought is expected for the future (Dai, 2013).
56 Increases in temperature variability also affect the intensity of heat waves (Schär et al., 2004). Extreme heat and drought
57 often co-occur (King et al. 2014), and soil water limitations can exacerbate the intensity of heat waves (Fischer et al.,
58 2007; Seneviratne et al., 2010) due to reduced evaporative cooling and increased sensible heat flux (Sheffield et al., 2012).
59 This combination of reduced water availability and increased evaporative demand places increased stress on terrestrial
60 ecosystems.

61

62 During summer 2012/2013, Australia experienced a record-breaking heat wave that was deemed unlikely without climate
63 change (Steffen, 2015). The Australian summer 2012/2013 was nicknamed the ‘Angry Summer’ or the ‘Extreme
64 Summer’, as an exceptionally extensive and long-lived period of high temperatures affected large parts of the continent in
65 late December 2012 and the first weeks of January 2013 (Bureau of Meteorology, BOM, 2013). Record temperatures were
66 observed in every Australian State and Territory, and the record for the hottest daily average temperature (32.4°C) for
67 Australia was recorded on the 8th of January (Karoly et al., 2013). On the Western Australian South Coast, the maximum
68 temperature record was broken in Eucla on the 3rd of January with 48.2°C. In South Australia maximum temperature
69 records were broken at four weather stations between the 4th and 6th of January. Victoria also observed record heat on the
70 4th of January at its south coast in Portland (42.1°C). In New South Wales, record temperatures were recorded on the 5th of
71 January and were broken again on the 19th, reaching 46.2°C before the heat wave subsided. Besides being the hottest year
72 since 1910, summer 2012/2013 was also considerably drier than average in most parts of the continent, but particularly in
73 the densely populated east of Australia. King et al. (2014) have shown that extreme heat was made much more likely by
74 contributions from the very dry conditions over the inland eastern region of Australia as well as by anthropogenic
75 warming.

76
77 Heat waves are becoming hotter, they last longer, and they occur more often (Steffen, 2015). As many ecological
78 processes are more sensitive to climate extremes than to changes in the mean state (Hanson et al. 2006), it is imperative to
79 understand the effect of climate extremes in order to predict the impact on terrestrial ecosystems. Processes and
80 sensitivities differ among biomes, but forests are expected to experience the largest detrimental effects and the longest
81 recovery times from climate extremes due to their large carbon pools and fluxes (Frank et al. 2015). There is increasing
82 evidence that climate extremes may result in a decrease in carbon uptake and carbon stocks (Zhao and Running, 2010,
83 Reichstein et al., 2013). It is therefore crucial to better understand ecosystem responses to climate extremes. The role of
84 climate extremes could be critical in shaping future ecosystem dynamics (Zimmermann et al. 2009), but the sporadic and
85 unpredictable nature of these events makes it difficult to monitor how they affect vegetation through space and time
86 (Mitchell et al., 2014).

87
88 Australian forest and woodland ecosystems are strongly influenced by large climatic variability, characterised by recurring
89 drought events and heat waves (Beringer et al., 2016, Mitchell et al., 2014). *Eucalyptus regnans* ecosystems in southeast
90 Australia, for example, have an exceptional capacity to withstand drought and the ability to recover almost instantly after
91 heat waves (Pfautsch and Adams, 2013). However, drought and heat related forest die-back events have been observed in
92 southwestern Australia (Matusick et al. 2013, Evans and Lyons 2013), where drought stress from long-term reductions in
93 rainfall have been exacerbated by short heat wave periods. This suggests that these ecosystems, even though they are
94 resilient to dry and hot conditions, are susceptible to mortality events once key thresholds have been exceeded (Evans et
95 al., 2013). Similar large-scale droughts and heat waves in Europe during 2003 (Ciais et al., 2005), in Canada during 2000

96 to 2003 (Kljun et al. 2007) and in the US during 2012 (Wolf et al. 2016) caused substantial reductions in summer carbon
97 uptake, and vegetation-climate feedbacks were found to contribute to enhanced temperatures (Teuling et al., 2010, Wolf et
98 al., 2016). However, direct observations of the ecosystem response to large-scale extremes in Australia have been lacking
99 until very recently.

100

101 The large spatial extent of the heat wave in early 2013 across Australia and direct observations from the OzFlux network
102 enable us for the very first time to analyse the effect of extreme hot and dry conditions on the carbon, water and energy
103 cycles of the major woodland and forest ecosystems across southern Australia. In this study, we combined eddy-
104 covariance measurements from seven woodland and forest sites with model simulations from BIOS2 (Haverd et al. 2013)
105 to investigate the impact of the 2012/2013 summer heat wave and drought on the carbon and water exchange of terrestrial
106 ecosystems across climate zones in southern Australia and to assess the influence of land-surface feedbacks on the
107 magnitude of the heat wave.

108 **2 Materials and Methods**

109 We compared hourly data from seven OzFlux sites (Fig. 1, Table 1) measured during the heat wave period 1 January 2013
110 – 18 January 2013 to observations from a background reference. We used eddy covariance data to compare hourly data
111 and the daily cycle of latent and sensible heat as well as carbon fluxes. We used the measured hourly data of a background
112 period (BGH) one year later from 2/1/2014 – 6/1/2014. During these time periods all towers were actively taking
113 measurements, although data gaps were present after 18 January in 2013. The reference period was shorter than the heat
114 wave period because another significant heat wave event affected southeastern Australia in late January 2014 during a
115 time period when not all sites had comparable data available in 2013. Temperatures during the background reference
116 period were also somewhat warmer than average climatology (Fig. 2). We therefore expect the relative severity of the
117 effects of the heat wave to appear smaller than they otherwise would when compared against a climatological reference.
118 To ensure the representativeness of our results, we also compared daily data against a climatology derived from daily
119 BIOS2 (see below) output for the time period 1982-2013 (background climatology, BGC). BIOS2 results for the whole
120 time period were only available as daily values.

121 **2.1 Sites**

122 We analysed data from seven southern Australian sites (Beringer et al., 2016) grouped in three distinct ecosystem and
123 climate types: Mediterranean woodlands (MW), temperate woodlands (TW) and temperate forests (TF) (Fig. 1, Table 1).

124

125 MW sites included i) a coastal heath *Banksia* woodland (Gingin: AU-Gin); ii) a semi-arid eucalypt woodland dominated
126 by Salmon gum (*Eucalyptus salmonophloia*), with Gimlet (*E. salubrious*) and other eucalypts (Great Western Woodlands:

127 AU-Gww); and iii) a semi-arid mallee ecosystem (Calperum: AU-Cpr), which is characterised by an association of mallee
128 eucalypts (*E. dumosa*, *E. incrassata*, *E. oleosa* and *E. socialis*) and spinifex hummocks (*Triodia basedowii*) (Sun et al.
129 2015, Meyer et al., 2015). TW sites are classified as dry sclerophyll woodlands and include: i) Wombat (AU-Wom), a
130 secondary re-growth of Messmate Stringybark (*E. oblique*), Narrow-Leaved Peppermint (*E. radiate*) and Candlebark (*E.*
131 *rubida*); ii) Whroo (AU-Whr), a box woodland mainly composed of Grey Box (*E. microcarpa*) and Yellow Gum (*E.*
132 *leucoxydon*) with smaller numbers of Ironbark (*E. sideroxylon*) and Golden Wattle (*Acacia pycnantha*); iii) Cumberland
133 Plains (AU-Cum), where the canopy is dominated by Gum-topped Box (*E. moluccana*) and Red Ironbark (*E. fibrosa*),
134 which host an expanding population of mistletoe (*Amyema miquelii*). Temperate Forests (TF) are represented by the
135 Tumbarumba site (AU-Tum), which is in a wet sclerophyll forest dominated by Alpine Ash (*E. delegatensis*) and
136 Mountain Gum (*E. dalrympleana*) (Leuning et al., 2005).

137
138 The sites fall into the classifications “Mediterranean Forests, Woodland and Scrub” (AU-Gin, AU-GWW and AU-Cpr) or
139 the “Temperate Broadleaf and Mixed Forest” (AU-Wom, Au-Cum, AU-Whr and AU-Tum) classifications of IBRA
140 (Interim Biogeographic Regionalisation for Australia v. 7; Environment, 2012). In temperate Australia both woodlands
141 and forests are mainly dominated by Eucalyptus species. Forests occur in the higher rainfall regions and woodlands form
142 the transitional zone between forests and grass-shrublands of the drier interior. We therefore classified temperate
143 ecosystems with mean annual precipitation > 1000 mm and tree height > 30 m as forests. There was only one temperate,
144 wet sclerophyll forest for which data was available during this heat wave, but we are confident that it is representative of
145 the energy limited temperate forests of southern Australia (e.g. van Gorsel, 2013). None of the sites is continental, but
146 elevations range from 33 m asl (AU-Cum) to 1260 m asl (AU-Tum). The mean annual temperature for the years 1982 -
147 2013 ranged from 9.8 °C in AU-Tum to 18.7°C in AU-Gww (Table 1). Mean annual precipitation also covered a large
148 range from 265 mm year⁻¹ in AU-Cpr to 1417 mm year⁻¹ in AU-Tum.

149 **2.2 OzFlux Data**

150 We analysed data collected by the OzFlux network (www.OzFlux.org.au). Each site has a set of eddy covariance (EC)
151 instrumentation, consisting of an infrared gas analyser (LI-7500 or LI-7500A, LI-COR, Lincoln, NE, USA) and a 3D
152 sonic anemometer (generally a CSAT3 (Campbell Scientific Instruments, Logan, UT, USA) except for AU-Tum, where a
153 Gill-HS is operational (Gill Instruments, Lymington, UK)). Supplementary meteorological observations include radiation
154 (4 component CNR4 or CNR1, Kipp and Zonen, Delft, Netherlands) and temperature and humidity (HMP45C or HMP50,
155 Vaisala, Helsinki, Finland). Soil volumetric water content was measured with CS616 (Campbell Scientific). EC data were
156 processed using the OzFlux-QC processing tool (Isaac et al., 2016). Processing steps and corrections included outlier
157 removal, coordinate rotation (double rotation), frequency attenuation correction, conversion of virtual heat flux to sensible
158 heat flux, and the WPL correction (Tanner and Thurtell, 1969, Wesley, 1970, Webb et al., 1980, Schotanus et al., 1983,
159 Lee et al. 2004 and references therein). Friction velocity thresholds were calculated following the method of Barr et al.

160 (2013). In Tumbarumba, where advection issues are known (van Gorsel et al., 2007, Leuning et al. 2008), only data from
161 the early evening was used during nighttime hours (van Gorsel, 2009). Gaps in the meteorological time series were filled
162 using alternate data sets, BIOS2 or ACCESS (Australian Community Climate and Earth-System Simulator) output (Bi et
163 al., 2013) or climatologies (usually in this order of preference). Gaps in the flux time series were filled using a self-
164 organising linear output model (SOLO-SOFM, Hsu et al., 2002, Abramowitz et al. 2006 and references therein). The
165 OzFlux data used in this analysis are available from <http://data.ozflux.org.au/portal/>.

166 **2.3 BIOS2**

167 The coupled carbon and water cycles were modelled using BIOS2 (Haverd et al., 2013a; Haverd et al., 2013b) constrained
168 by multiple observation types, and forced using remotely sensed vegetation cover and daily AWAP meteorology
169 (Raupach et al. 2009), downscaled to half-hourly time resolution using a weather generator. BIOS2 is a fine-spatial-
170 resolution (0.05 degree) offline modelling environment, including a modification of the CABLE biogeochemical land
171 surface model (Wang et al., 2011; Wang et al., 2010) incorporating the SLI soil model (Haverd and Cuntz, 2010). BIOS2
172 parameters are constrained and predictions are evaluated using multiple observation sets from across the Australian
173 continent, including streamflow from 416 gauged catchments, eddy flux data (CO₂ and H₂O) from 14 OzFlux sites
174 (Haverd et al., 2016), litterfall data, and soil, litter and biomass carbon pools (Haverd et al., 2013a). In this work, we
175 updated BIOS2 to use the GIMMS3g FAPAR product (Zhu et al., 2013) instead of MODIS and AVHRR products for
176 prescribed vegetation cover (Haverd 2013b). The reference period used for BIOS2 (BGC), was 1982-2013, the period over
177 which remotely sensed data were available.

178 **2.4 Analyses**

179 All data analyses were performed on Jupyter notebooks using Python 2.7.11 and the Anaconda (4.0.0) distribution by
180 Continuum Analytics. Differences between heat waves and reference periods were determined by calculating z-scores of
181 temperatures and soil water content during the relevant periods. z-scores represent the number of standard deviations an
182 observation is above or below the mean, depending upon the sign of the z-score. These were calculated with the z-score
183 function of the scipy stats module for the period 1st–18th January relative to the mean across all years in the BIOS2 output
184 (1982-2013). The scipy stats functions bartlett and ttest_ind were used to determine the significance of differences of a
185 range of variables between the background period (BGH or BGC) and the heat wave periods HW1 (1/1/2013–9/1/2013)
186 and HW2 (HW2, 10/1/2013–18/1/2013). Boxplots were created using Matplotlib.

187 **2.5 Conventions**

188 We use the terminology and concepts as introduced by Chapin et al. (2006), where net and gross carbon uptake by
189 vegetation (net ecosystem production (NEP) and gross primary production (GPP)) are positive directed toward the surface

190 and carbon loss from the surface to the atmosphere (ecosystem respiration (ER)) is positive directed away from the
191 surface.

192 **3 Results**

193 **3.1 Heat wave characterisation**

194 The heat wave event commenced on the 25th of December 2012 with a build-up of extreme heat in the southwest of
195 Western Australia. A high pressure system in the Great Australian Bight and a trough near the west coast directed hot
196 easterly winds over the area (BOM, 2013). From December 31 the high pressure system started moving eastward, and it
197 entered the Tasman Sea off eastern Australia on January 4th. The northerly winds directed very hot air into south eastern
198 Australia. Temporary cooling was observed in the eastern states after the 8th of January, but a second high pressure system
199 moved into the Bight in the meantime, starting a second wave of record breaking heat across the continent. The heat wave
200 finally ended on the 19th of January, when southerly winds brought cooler air masses to southern Australia.

201

202 Figure 3 shows the meteorological conditions at the sites during the heat wave. Maximum temperatures as high as 46.3°C
203 were accompanied by vapour pressure deficits up to 9.7 kPa. The soil water fraction was as low as 0.02 in MW but
204 increased to 0.05 and 0.4 at AU-Gin and AU-Gww respectively after synoptic rainfalls around the 12th of January. The
205 same, but less pronounced, was also the case for the TW sites where soil water fractions increased from 0.10 to 0.18 after
206 rain. At the TF site, Au-Tum, soil water content decreased throughout the heat wave (HW) from 0.26 to 0.19. Due to
207 intermittent precipitation events we analysed two parts of the heat wave separately: heat wave period 1 (HW1, 1st–9th of
208 January 2013) was characterised by very little precipitation (2 mm over all sites) and low soil water content. During heat
209 wave period 2 (HW2, 10th–18th of January 2013) precipitation occurred at most sites (12th–15th January 2013) and resulted
210 in increased soil water content at some sites and lower temperature anomalies at all sites than during HW1.

211

212 During HW1 temperatures were generally more than 1.5-2 standard deviations (σ) higher than the 32-year mean of the
213 background period (BGC) for these dates. At AU-Tum and AU-Gww z-scores exceeded $+2\sigma$. During HW2 all sites
214 showed lower z-scores for temperature, but they were still more than $+1\sigma$ higher than average background temperatures.
215 The background period BGH, against which we compare the hourly data of the heat wave, was also warmer than average
216 conditions during the past 30 years, but these z-scores were well below 1 for most sites.

217

218 Z-values indicate that soil water content was unusually low for the time of year. It was mostly more than one standard
219 deviation below average ($\sigma < -1$), except at AU-Gww where soil water content was higher than average during HW2. All
220 sites except AU-Gin and AU-Gww had a lower z-score for soil water content during HW2 than HW1, indicating relatively
221 drier conditions with respect to the BIOS2 derived climatology despite the presence of rainfall during HW2. The

222 background period BGH was generally less dry than the heat wave periods, one noteworthy exception being AU-Tum,
223 which had very dry conditions (-2σ) in BGC during early January 2014. The z-scores indicate that high temperatures were
224 more unusual than low soil water content during HW1. HW2 was both hot and dry.

225 **3.2 Ecosystem response to dry and hot conditions**

226 **3.2.1 Energy Exchange**

227 Incoming and reflected short-wave radiation were significantly increased by only 70 Wm^{-2} and 3 Wm^{-2} respectively in the
228 energy limited ecosystem AU-Tum during the first period of the heat wave (Fig. 4, Table 2). Otherwise they remained
229 approximately the same as BGH values except at the MW sites where they were significantly reduced (by -62 Wm^{-2})
230 during HW2 (Table 2). The relatively short duration of the extreme heat wave did not result in changes to albedo (not
231 shown). A warmer atmosphere and potentially increased cloud cover led to a 38 Wm^{-2} increase in longwave downward
232 radiation in Western Australia. Due to increased surface temperatures, longwave radiation emitted at the land surface was
233 significantly increased at all sites for both heat wave periods (28 Wm^{-2} on average), but more so during HW1 (41 Wm^{-2} on
234 average). Net radiation was significantly reduced during HW2, but only at MW sites (-35 Wm^{-2}). At all other sites, net
235 radiation was approximately the same during HW1, HW2 and BGH. Available energy (not shown), the energy available
236 to the turbulent heat fluxes, was significantly reduced at MW and TW sites during HW1 (by 25 Wm^{-2} and 24 Wm^{-2}
237 respectively) but was about the same for HW2. It was also about the same during HW1 and HW2 at the TF site.

238
239 Figure 5 demonstrates how remarkably different the energy partitioning was at MW, TW and TF sites, as we would expect
240 given their large climatological and biogeographic differences (Beringer et al., 2016). While similar fractions of energy
241 went into latent and sensible heat at the TF site, more energy was directed into sensible heat at TW sites. This energy flux
242 partitioning toward sensible heat was more pronounced at MW sites, where both the mean and the variability of latent heat
243 flux were very small due to severe water limitations. Most of the available energy was transferred as sensible heat and
244 hence contributed to the warming of the atmosphere which was also observed for BGH.

245
246 During HW1, the generally small latent heat flux at the MW sites (38 Wm^{-2}) was further reduced by -12 Wm^{-2} (Table 2).
247 During HW2, precipitation temporarily increased water availability, returning latent heat flux to levels observed during
248 BGH. Latent heat flux did not change significantly at TW sites during the HWs compared to BGH conditions. At TF,
249 however, latent heat flux increased by 52 and 14 Wm^{-2} during HW1 and HW2 respectively. This was partly due to the
250 very dry conditions in the background period BGH, but daily latent heat flux was also increased compared to the
251 climatology (BGC, Fig. A2), particularly during HW1.

252

253 With values exceeding 7, the observed ratio of sensible to latent heat, the Bowen ratio (β , Bowen, 1926), was very large in
254 the Mediterranean woodlands (Fig. 6). Typical values for β reach 6 for semi-arid to desert areas (e.g. Oliver, 1987,
255 Beringer and Tapper, 2000). During the heat wave these values were larger than 10. With rainfall and increased latent heat
256 flux, β decreased to below background conditions in HW2 (6.4) across the MW sites. At TW, β was higher than
257 background values during HW1 (reaching a maximum value of 4.0) but decreased to background values during HW2
258 (2.8). For the TF site, β was lower (0.7 and 0.8 during HW1 and HW2 respectively) than during the background period
259 (1.0). It increased steadily in the morning, declined toward the evening and was quite symmetric, while in TW β increased
260 strongly in the afternoon during the heat waves. This increase of β toward the afternoon hours was observed in MW
261 during all time periods (including BGH).

262
263 Measured daily latent heat fluxes and β were consistent with flux climatology derived from BIOS2 during the background
264 (BGC) (Fig. A1).

265 **3.2.2 Carbon Exchange**

266 Patterns of carbon fluxes were similar to between-site patterns of energy fluxes (Fig. 7, note differences in y-axes). All
267 sites showed that maximum carbon uptake (GPP) occurred in the morning, decreased throughout the afternoon, and
268 mostly increased again in the late afternoon. NEP followed the diurnal course of GPP, with the offset related to total
269 ecosystem respiration (ER). ER increased with temperature and reached a maximum in the early afternoon (not shown).
270 Maximum NEP at MW decreased from $4.16 \mu\text{mol m}^{-2} \text{s}^{-1}$ during background conditions to $2.2 \mu\text{mol m}^{-2} \text{s}^{-1}$ in HW1 and
271 $3.3 \mu\text{mol m}^{-2} \text{s}^{-1}$ in HW2. Not only did the total amount of carbon uptake decrease, but the number of hours during which
272 the ecosystem was sequestering carbon also decreased from 11.5 hours in background conditions to 10.5 during HW1 and
273 9.0 in HW2. The same was true in TW and TF in that maximum NEP was lower during the heat wave periods and the
274 time during which the ecosystems acted as sinks was shortened.

275
276 Carbon uptake was significantly reduced at MW and TW during HW1 (Fig. 8) with daytime averages decreasing from 4.6
277 $\mu\text{mol m}^{-2} \text{s}^{-1}$ to 3.1 in MW and from 11.2 to $6.2 \mu\text{mol m}^{-2} \text{s}^{-1}$ in TW. In TF, however, carbon uptake was increased from
278 $24.2 \mu\text{mol m}^{-2} \text{s}^{-1}$ to $26.5 \mu\text{mol m}^{-2} \text{s}^{-1}$ during HW1 and to 27.0 during HW2. Ecosystem respiration increased significantly
279 in both periods of the heat wave and across all ecosystems. Consequently, NEP was significantly reduced at MW and TW
280 sites during both heat wave periods, unchanged at the TF site during HW1, but increased at TF during HW2. During
281 daytime all ecosystems remained carbon sinks during the event but as there were fewer hours and decreased carbon uptake
282 during the day the woodlands switched into carbon sources. Precipitation after HW1 and cooler temperatures during HW2
283 led to a recovery of the carbon sink in TW during HW2. TF was a strong sink of carbon and remained so during both HW
284 periods.

285

286 Measured GPP and ER showed the same responses in carbon uptake and losses during the heat waves as the flux
287 climatology derived with BIOS2 (BGC, Fig. A2): GPP was reduced during HW1 in woodland ecosystems and increased
288 in the forest during both heat wave periods. ER was increased at all sites and during HW1 and HW2 compared to the long-
289 term climatology.

290 **4 Discussion**

291 **4.1 Consequences of Australian heat waves on energy fluxes**

292 Persistent anticyclonic conditions during the 'Angry Summer of 2012/13' led to a heat wave by transporting warm air
293 from the interior of the continent to southern Australia. Such synoptic conditions are the most common weather pattern
294 associated with Australian heat waves (Steffen et al., 2014). However, these weather patterns did not result in increased
295 amounts of available energy at the surface, which was in contrast to heat waves observed in Europe and the US (see
296 section 4.4). Instead, in our study the energy available for turbulent heat fluxes was similar to or even smaller than
297 background conditions. Background conditions over Australia tend to have large available energy fluxes, even during very
298 cyclonic periods (e.g., the 2010–2011 fluvial; Cleverly et al. 2013). Thus, differences in latent and sensible heat fluxes at
299 the Australian sites used in this study were due to anomalous temperature and soil moisture content rather than to changes
300 in available energy.

301

302 During the heat wave, available energy preferentially increased sensible heat flux and led to a subsequent increase of β at
303 drier sites (MW and TW) while at the TF site, available energy preferentially increased latent heat flux. The diurnal cycle
304 of β at the MW sites generally showed an increase of β toward the afternoon hours. This increase was more pronounced
305 during the heat wave periods than during BGH, indicating stress-induced reduction of stomatal conductance (Cowan and
306 Farquhar 1977). At TW sites, β only had a pronounced asymmetry during heat waves, clearly showing stronger stomatal
307 control than during background conditions. At the TF site, β was lower during heat waves, but the symmetry in β indicates
308 that a decrease in midday stomatal conductance was either counteracted by increased soil evaporation under a steadily
309 increasing humidity deficit with rising temperatures from morning to mid-afternoon (Tuzet et al. 2003), or that there was
310 little stomatal control of the latent heat flux at this site, or a combination of both. Stomatal closure and the associated
311 partitioning of available energy is important as an increased β in response to heat waves (MW and TW) promotes further
312 heating of the atmosphere, whereas increased latent heat flux suppresses further atmospheric heating (Teuling et al.,
313 2010). This is only possible as long as the latent heat flux is not limited by soil water, particularly during the period of
314 peak insolation (Wolf et al. 2016). At TF the relative extractable water was above a threshold of 0.4 (J. Suzuki, pers.
315 comm.) for all but the last two days of the heat wave (not shown), indicating that for most of the time soil water was not

316 limiting the latent heat flux (Granier et al., 1999). Thus, evaporative cooling from latent heat suppressed further heating
317 but depleted soil moisture at the TF site. Eventually, depleted soil water stores can lead to a positive (enhancing) feedback
318 on temperatures as more energy goes into the sensible than the latent heat flux further amplifying heat extremes by
319 biosphere–atmosphere feedback (Whan et al. 2015). Indeed, the data indicate that toward the end of the heat wave, such
320 positive feedbacks had shifted energy partitioning toward sensible heat flux at all sites.

321 **4.2 Impact of heat waves on carbon fluxes**

322 Heat waves and drought can affect photosynthesis (Frank et al., 2015). By means of stomatal regulation, plants exert
323 different strategies to balance the risks of carbon starvation and hydrological failure (Choat et al. 2012). These strategies
324 particularly come into play during extreme events (Anderegg et al. 2012). While the ecosystem response during heat
325 waves is linked to plant stress from excessively high temperatures and increased evaporative demand (i.e. higher vapour
326 pressure deficit), drought stress occurs when soil water supply can no longer meet the plant evaporative demand. The
327 former will lead to reduced carbon uptake through e.g. stomatal closure and disruptions in enzyme activity, the latter can
328 have direct impacts on carbon uptake by reducing stomatal and mesophyll conductance, the activity and concentrations of
329 photosynthetic enzymes (Frank et al., 2015 and references therein). Apart from these almost instantaneous responses
330 additional lagged effects can further impact the carbon balance. If high temperatures were to occur in isolation we would
331 expect to observe a decrease in GPP. During the 2012/2013 heat waves in Australia, we observed a diurnal asymmetry in
332 GPP at all sites and in all measurement periods. This is expected in ecosystems that exert some degree of stomatal control
333 to avoid excessive reductions in water potential (e.g. in the afternoon), during higher atmospheric demand and when there
334 is a reduced ability of the soil to supply this water to the roots because of lower matrix potentials and hydraulic
335 conductivity (Tuzet et al. 2003). Daily average carbon uptake at MW and TW was reduced by up to 32% and 40%,
336 respectively. At the TF site, however, daily averaged carbon uptake did not change significantly, and daytime carbon
337 uptake was significantly increased during both periods of the heat wave (see also Fig. 7). This can be explained partly by
338 the very dry conditions during the background period at this site, which could also have caused below average carbon
339 uptake, although comparing the site data against the long-term climatology confirmed an increased carbon uptake during
340 the heat wave (not shown). Although air temperatures clearly exceeded the ecosystem scale optimum of 18°C for carbon
341 uptake, and vapour pressure deficit exceeded values of 12 hPa, where stomatal closure can be expected at this site (van
342 Gorsel et al. 2013), increased incoming shortwave radiation (Tab. 2) more than compensated for these factors with
343 increased carbon uptake in this typically energy limited ecosystem during the heat wave. Overall, we have observed a
344 strong contrast between the water and energy limited ecosystems with the former (MW and TW) having strongly reduced
345 GPP during heat waves and the latter (TF) having equal or slightly larger GPP.

346

347 Heat waves and drought not only affect photosynthesis but also have an impact on respiration (Frank et al., 2015).
348 Increases in ER during the heat wave seem intuitive, given the exponential response of respiration to temperature (e.g.
349 Richardson et al., 2006). Drought can also override the positive effect of warmer temperatures and lead to reduced
350 respiration due to water limitations, as observed during the 2003 heat wave (Reichstein et al., 2007) or the 2011 spring
351 drought (Wolf et al. 2013) in Europe. However, during the observed heat waves in Australia, increased air and soil
352 temperatures led to significantly increased ecosystem respiration at all sites, indicating that the thermal response of
353 respiration was undiminished despite soil moisture deficits.

354
355 While all sites remained carbon sinks during daytime hours in both heat wave periods, reduced carbon uptake in the
356 woodlands turned them to a net a source of carbon on a daily average. It can hence be concluded that increased ER
357 combined with decreased or unchanged GPP likely turned large areas of Southern Australia from carbon sinks to sources.
358 Unlike the Mediterranean woodlands, the temperate woodlands recovered quickly after rain but the response of these
359 ecosystems to a short though intense heat wave indicates that future increases in the number, intensity and duration of heat
360 waves can potentially turn the woodlands into carbon sources, leading to a positive carbon-climate feedback. Heat waves
361 can also induce a transition from energy-limited to water-limited ecosystems (Zscheischler et al. 2015). Transitioning
362 toward water limitation, especially for energy-limited forests, can exacerbate the detrimental effects of extreme events.
363 Recurrent non-catastrophic heat stress can also lead to increased plant mortality, the impact of which would be more
364 evident over longer timescales (McDowell et al., 2008) and as an increase in the frequency of fires (Hughes, 2003).
365 Similarly, legacy or carry-over effects of drought result in increased mortality and shifts in species composition during
366 subsequent years (van der Molen et al. 2011). Future climate change is likely to be accompanied by increased plant water
367 use efficiency due to elevated CO₂ (Keenan et al., 2013), which could lead to more drought and heat resilient plants, but
368 also to ecosystems with higher vegetation density and thus both higher water demands (Donohue et al., 2013, Ukkola et
369 al., 2015) and a greater susceptibility to large fires (Hughes, 2003). Furthermore, changes in the prevalence of drought will
370 affect forest carbon cycling and their feedbacks to the Earth's climate (Schlesinger et al. 2016). For Australia, there is
371 evidence that semi-arid ecosystems have a substantial influence on the global land carbon sink (Poulter et al 2014,
372 Ahlström et al. 2015). Due to their impact on the global carbon cycle, predicting the future influence of heat waves and
373 drought on the land sink of Australian woodlands thus remains a key research priority.

374 **4.3 The effect of intermittent precipitation during the heat wave**

375 Intervening rain events led to differentiated responses in energy fluxes and lower air temperatures, but soil moisture
376 content remained mostly low during HW2 (see section 3.1). Available energy was significantly lower (compared to BGH)
377 during HW2 at MW but remained similar at TW and TF. At TF the latent heat flux in HW2 was still enhanced compared
378 to BGH yet smaller than during HW1. Following rainfall the energy partitioning at the MW sites changed toward latent

379 heat flux, with fractions similar to or larger than background conditions. This indicates that soil moisture feedbacks which
380 inhibit warming of the lower atmosphere largely led to a return to standard conditions. At TW, β decreased to background
381 values when precipitation occurred. While the magnitude returned to values similar to BGH, there was still a noticeable
382 increase of β in the afternoon hours that was more pronounced than under average conditions. An increased fraction of
383 energy going into the latent rather than the sensible heat during HW2 at the drier sites (MW and TW) does not only have
384 important consequences on the soil moisture–temperature feedback but also on ameliorating vapour pressure deficit (Fig.
385 3) and reducing the atmospheric demand that acts as a stressor on plants (Sulman, et al. 2016).

386
387 During HW1, the time of maximum carbon uptake at the woodland sites was earlier in the morning than during BGH, and
388 we observed strongly reduced carbon uptake throughout the day. During HW2, however, the shift of maximum GPP
389 toward earlier hours of the day was less pronounced at MW and TW, thus daytime carbon uptake was not significantly
390 reduced. This was in response to the intermittent precipitation and lower temperatures, which led to a reduction in vapour
391 pressure deficit and increased soil water availability. Increased ER at all sites and during both HW periods was dominated
392 by warmer temperatures more than soil moisture limitations. Increased ER combined with decreased or unchanged GPP
393 likely turned large areas of Southern Australia from carbon sinks to sources, an effect that was reduced but not offset by
394 the intermittent precipitation.

395
396 When carbon losses exceed carbon gains over a long time period (e.g. through increased respiration) mortality can result
397 as a consequence of carbon starvation. Eamus et al. (2013) identified increased vapour pressure deficit as detrimental to
398 transpiration and net carbon uptake, finding that increased vapour pressure deficit is more detrimental than increased
399 temperatures alone - with or without the imposition of drought. A recent study by Sulman et al. (2016) confirmed that
400 episodes of elevated vapour pressure deficit could reduce carbon uptake regardless of changes in soil moisture. Here, all
401 ecosystems responded with increased carbon uptake to the precipitation events and the associated lower temperatures and
402 vapour pressure deficit. The improved meteorological conditions thus likely decreased the risk of mortality during HW2.
403 As heat waves increase in frequency, duration and intensity in the future (Trenberth et al. 2014), however, we expect a
404 decline in the ameliorating effects of intermittent rain events and an increased risk of mortality.

405 **4.4 Comparisons to other heat waves (Europe, N America, China)**

406 Anticyclonic conditions also caused the intense 2003 European heat wave (Black et al., 2004) as well as the even more
407 intense and widespread heat wave that reached across Eastern Europe, including western Russia, Belarus, Estonia, Latvia,
408 and Lithuania in 2010 (Dole et al. 2011). Less cloud cover and more clear sky conditions strongly increased incoming
409 radiation and available energy during the European heat wave and drought in 2003 (Teuling et al., 2010), as well as during

410 the recent drought and heat in California (Wolf et al., in revision), in contrast to the current study. Teuling et al. (2010)
411 observed that surplus energy led to increases in both latent and sensible heat fluxes: over grassland, the energy was
412 preferentially used to increase the latent heat flux, thereby decreasing β , whereas forest ecosystems generally had a
413 stronger increase in the sensible heat flux and an increase in β (Teuling et al. 2010, van Heerwaarden & Teuling 2014).
414 These results highlight the important ecosystem services provided by forests in the long-term, particularly considering the
415 increased prevalence of droughts and temperature extremes projected in the future (Trenberth et al. 2014). The situation in
416 our study was somewhat different in that soil water was only briefly limited in TF, where latent heat flux was mainly
417 driven by temperature and vapour pressure deficit. After an intervening period of precipitation latent heat flux increased at
418 the drier sites (MW, TW) while sensible heat flux decreased or remained the same, potentially breaking the soil moisture–
419 temperature feedback loop in Australia that maintained the heat wave in 2003 Europe. These findings highlight the
420 important role of Australian forest and woodland ecosystems in mitigating the effects of heat waves.

421
422 Stomatal control and reductions in GPP at the dry sites (MW and TW) were consistent and of similar magnitude with
423 observations made during e.g. the 2003 European heat wave (Ciais et al. 2005), the 2010 European heat wave (Guerlet,
424 2013), the 2012 US drought (Wolf et al. 2016), and the 2013 heat wave and drought that affected large parts of Southern
425 China (Yuan et al. 2015). During these heat waves and droughts, carbon uptake was strongly reduced in general and
426 biosphere–atmosphere feedbacks from reduced vegetation activity further enhanced surface temperatures. This contrasts
427 with the wet site (TF), where local drought effects were observed only toward the end of the study. We found that the
428 response of carbon fluxes of Australian woodland (dry) ecosystems were similar to comparable heat waves on other
429 continents, whereas the detrimental effects of the heat wave were largely ameliorated in wet, energy-limited Australian
430 ecosystems.

431
432 Temperature anomalies during the 2012/2013 heat wave in Australia were less extreme ($\leq -2 \sigma$, Fig. 2) than during the
433 2010–2011 heat waves in Texas and Russia (-3σ) and the 2003 European heat wave ($> 2 \sigma$) (Hansen et al., 2012; Bastos
434 et al., 2014), which resulted in smaller ecosystem responses than in Europe (Reichstein et al., 2007). However, this does
435 not imply that Australian heat waves are less severe than their Northern Hemisphere counterparts because background
436 variability in climate, weather and ecosystem productivity are larger in Australia due to periodic synchronisation of El
437 Niño–Southern Oscillation, the Indian Ocean dipole and the state of the southern annular mode (Cleverly et al., 2016a).
438 When these climate modes are in phase, continental heat waves are strongly related to drought and reduced soil water
439 content, although not to the same extent as in Europe during 2003 (Perkins et al., 2015). Nonetheless, responses of
440 Australian vegetation to heat waves and drought are consistent with vegetation responses elsewhere. For example during
441 the 2003 European heat wave, productivity in grasslands was most sensitive to heat and drought, while open shrublands
442 and evergreen broadleaf forests (like those in our study) were the least sensitive (Zhang et al., 2016). Two-thirds of the
443 productivity in Australia is due to CO₂ uptake in non-woody ecosystems (Haverd et al., 2013), and it was indeed the semi-

444 arid grasslands that produced the extraordinary CO₂ source strength during the drought and heat wave of January 2013
445 (Cleverly et al., 2016b). Similarly, the semi-arid Mulga woodlands responded to the 2012/2013 heat wave with a large net
446 source strength, increase in ecosystem respiration and afternoon depression in GPP (Cleverly et al., 2016b). We
447 demonstrated in this study that *Eucalypt* forest and woodland ecosystems of southern Australia were more sensitive to
448 heat waves if those ecosystems also experience moisture limitations.

449 **5 Conclusion**

450 We have shown that extreme events such as the ‘Angry Summer’ 2012 / 2013 can alter the energy balance and therefore
451 dampen or amplify the event. During this event the woodland sites reduced latent heat flux by stomatal regulation in
452 response to the warm and dry atmospheric conditions. Stronger surface heating in the afternoons then led to an
453 amplification of the surface temperatures. Only the forest site AU-Tum had access to readily available soil water and
454 showed increased latent heat flux. The increased latent heat flux mitigated the effect of the heat wave but continuously
455 depleted the available soil water. The generally increased atmospheric and soil temperatures led to increased respiration
456 but unchanged net ecosystem productivity. The woodlands turned from carbon sinks into carbon sources and while the
457 temperate woodlands recovered quickly after rain, the Mediterranean woodlands remained carbon sources throughout the
458 duration of the heat wave. This demonstrates that there is potential for positive carbon – climate feedbacks in response to
459 future extreme events, particularly if they increase in duration, intensity or frequency.

460

461 **Appendix A**

462 We have used measurements of a reference period during the same season but one year after the heat wave 2012 / 2013
463 occurred. Ideally we would have used a climatology derived from observations but OzFlux is a relatively young flux
464 tower network. The first two towers started in 2001 and even globally, very few flux towers have been measuring for
465 more than 15 years, which is relatively short compared to typical climatology records of 30-years. To ensure the
466 representativeness of our results we have therefore compared daily data against a climatology derived from BIOS2 output
467 for the time period 1982-2013.

468 Table A1 shows the agreement between BIOS2 output for all sites and the time period the year 2013. Agreement was
469 generally very good, even more so for the latent heat flux than for the carbon fluxes. Carbon fluxes, and more specifically
470 respiration at the dry Mediterranean woodlands showed stronger disagreement. It is likely that this to some degree reflects
471 night time issues with the eddy covariance method (e.g. van Gorsel, 2009) and with the partitioning of the measured
472 fluxes. This may also be an indication that the model was underestimating drought-tolerance at these sites. The low
473 modelled carbon uptake corresponded to periods of low soil water. There were long periods when the modelled soil water

474 was below wilting point within the entire root zone of 4m. Underestimation could occur if roots were accessing deeper
475 water, the wilting point parameter was too high or the modelled soil water was too low, relative to the wilting point.
476 Figure A1 shows that during HW1 the latent heat flux at the MW and TW sites was reduced. During HW2, precipitation
477 and temporarily increased water availability brought the latent heat flux back to levels observed during BGH for the
478 woodland sites. At the temperate forest, however, the latent heat flux strongly increased, particularly during HW1.
479 Increasingly reduced soil water and lower temperatures reduced the effect during HW2.
480 Figure A2 shows that carbon uptake was decreased at MW and TW during HW1 and similar to background conditions
481 during HW2. At TF, the forest site, carbon uptake was increased. Respiration (Fig. A2b) was increased at all locations and
482 during both heat wave periods.

483 **Acknowledgements**

484 This work utilised data from the OzFlux network which is supported by the Australian Terrestrial Ecosystem Research
485 Network (TERN) (<http://www.tern.org.au>) and by grants funded by the Australian Research Council. We would like to
486 acknowledge the contributions Ray Leuning made to OzFlux and Au-Tum. Ray has been cofounder and leader of the
487 OzFlux community and has been a great mentor to many in our network. We would also like to acknowledge the strong
488 leadership role that Helen Cleugh had over many years. The network would not be where it is without their input. VRD
489 and EP acknowledge the Education Investment fund and HIE for construction and maintenance of the AU-Cum tower.
490 The Australian Climate Change Science Program supported contributions by EvG and VH, SW was supported by the
491 European Commission's FP7 (Marie Curie International Outgoing Fellowship, grant 300083) and ETH Zurich. VRD
492 acknowledges funding from a Ramón y Cajal fellowship RYC-2012-10970. NK acknowledges funding from The Royal
493 Society UK, Grant IE110132. We would further like to acknowledge the referees and their helpful comments that have
494 helped us to improve this manuscript.

495 **References**

496 Ahlström, A., Raupach, M. R., Schurgers, G., Smith, B., Arneth, A., Jung, M., Reichstein, M., Canadell, J. G.,
497 Friedlingstein, P., Jain, A. K., Kato, E., Poulter, B., Sitch, S., Stocker, B. D., Viovy, N., Wang, Y. P., Wiltshire, A.,
498 Zaehle, S., and Zeng, N.: The dominant role of semi-arid ecosystems in the trend and variability of the land CO₂ sink,
499 *Science*, 348, 895-899, 2015.
500
501 Anderegg, W. R. L., Berry, J. A., Smith, D. D., Sperry, J. S., Anderegg, L. D. L., and Field, C. B.: The roles of hydraulic
502 and carbon stress in a widespread climate-induced forest die-off, *Proceedings of the National Academy of Sciences*, 109,
503 233-237, 2012.

504

505 Abramowitz, G., Gupta, H., Pitman, A.J., Wang, Y.P., Leuning, R., Cleugh, H. and Hsu, H.-L.: Neural Error Regression
506 Diagnosis (NERD): A tool for model bias identification and prognostic data assimilation, *J Hydrometeor*, 7, doi:
507 10.1175/JHM479.1, 2006.

508

509 Barr, A. G., Richardson, A. D., Hollinger, D. Y., Papale, D., Arain, M. A., Black, T. A., Bohrer, G., Dragoni, D., Fischer,
510 M.L., Gu, L., Law, B.E., Margolis, H.A., McCaughey, J.H., Munger, J.W. , Oechel, W. , Schaeffer, K.: Use of change-
511 point detection for friction–velocity threshold evaluation in eddy-covariance studies, *Agr Forest Meteorol*, 171,
512 doi:10.1016/j.agrformet.2012.11.023, 2013.

513

514 Bastos, A, Gouveia, CM, Trigo, RM, and Running, SW: Analysing the spatio-temporal impacts of the 2003 and 2010
515 extreme heatwaves on plant productivity in Europe, *Biogeosciences*, 11, 3421-3435, doi: 10.5194/bg-11-3421-2014, 2014.

516

517 Beringer, J. and Tapper, N. J.: The influence of subtropical cold fronts on the surface energy balance of a semi-arid site, *J.*
518 *Arid Environ*, doi:10.1006/jare.1999.0608, 2000.

519

520 Beringer, J., Hutley, L.B., McHugh, I., Arndt, S.K., Campbell, D., Cleugh, H.A., Cleverly, J., Resco de Dios, V., Eamus,
521 D., Evans, B., Ewenz, C., Grace, P., Griebel, A., Haverd, V., Hinko-Najera, N., Huete, A., Isaac, P., Kannia, K., Leuning,
522 R., Liddell, M.J., Macfarlane, C., Meyer, W., Moore, C., Pendall, E., Phillips, A., Phillips, R.L., Prober, S., Restrepo-
523 Coupe, N., Rutledge, S., Schroeder, I., Silberstein, R., Southall, P., Sun, M., Tapper, N.J., van Gorsel, E., Vote, C.,
524 Walker, J. and Wardlaw., T.: An introduction to the Australian and New Zealand flux tower network - OzFlux.
525 *Biogeosciences Discuss.*, accepted for publication, 2016.

526

527 Bi, D., Dix, M., Marsland, S., O'Farrell, S., Rashid, H., Uotila, P., Hirst, A., Kowalczyk, E., Golebiewski, M., Sullivan,
528 A., Yan, H., Hannah, N., Franklin, C., Sun, Z., Vorralik, P., Watterson, I., Zhou, X., Fiedler, R., Collier, M., Ma, Y.,
529 Noonan, J., Stevens, L., Uhe, P., Zhu, H., Griffies, S., Hill, R., Harris, C. and Puri, K: The ACCESS coupled model:
530 description, control climate and evaluation, *Australian Meteorological and Oceanographic Journal*, 63, 41-64, 2013.

531

532 Black, E., Blackburn, M., Harrison, G., Hoskins, B., Methven, J.: Factors contributing to the summer 2003 European heat
533 wave, *Weather* 59, 217–223, 2004.

534

535 Bowen, I. S.: The ratio of heat losses by conduction and by evaporation from any water surface., *Phys. Rev.*, 27, 779–787,
536 1926.

537

538 Bureau of Meteorology: Extreme heat in January 2013. Special Climate Statement 43 , Melbourne. Retrieved from
539 www.bom.gov.au/climate/current/statements/scs43e.pdf, 2013.

540

541 Chapin, F. S., Woodwell, G. M., Randerson, J. T., Rastetter, E. B., Lovett, G. M., Baldocchi, D. D., Clark, D. a., Harmon,
542 M.E., Schimel, D. S., Valentini, R., Wirth, C.,Aber, J. D., Cole, J. J., Goulden, M. L., Harden, J. W., Heimann, M.,
543 Howarth, R.W., Matson, P. a., McGuire, a. D., Melillo, J. M., Mooney, H. a., Neff, J. C., Houghton, R. a., Pace, M. L.,
544 Ryan, M. G.,Running, S. W., Sala, O. E., Schlesinger, W. H. and Schulze, E.-D. D.: Reconciling Carbon-cycle Concepts,
545 Terminology, andMethods, *Ecosystems*, 9(7), 1041–1050, doi:10.1007/s10021-005-0105-7, 2006.

546

547 Choat, B., Jansen, S., Brodribb, T. J., Cochard, H., Delzon, S., Bhaskar, R., Bucci, S. J., Feild, T. S., Gleason, S. M.,
548 Hacke, U. G., Jacobsen, A. L., Lens, F., Maherali, H., Martinez-Vilalta, J., Mayr, S., Mencuccini, M., Mitchell, P. J.,
549 Nardini, A., Pittermann, J., Pratt, R. B., Sperry, J. S., Westoby, M., Wright, I. J., and Zanne, A. E.: Global convergence in
550 the vulnerability of forests to drought, *Nature*, 491, 752-755, 2012.

551

552 Ciais, P., Reichstein, M., Viovy, N., Granier, A., Ogee, J., Allard, V., Aubinet, M., Buchmann, N., Bernhofer, C., Carrara,
553 A., Chevallier, F., De Noblet, N., Friend, A. D., Friedlingstein, P., Grunwald, T., Heinesch, B., Keronen, P., Knohl, A.,
554 Krinner, G., Loustau, D., Manca, G., Matteucci, G., Miglietta, F., Ourcival, J. M., Papale, D., Pilegaard, K., Rambal, S.,
555 Seufert, G., Soussana, J. F., Sanz, M. J., Schulze, E. D., Vesala, T., and Valentini, R.: Europe-wide reduction in primary
556 productivity caused by the heat and drought in 2003, *Nature*, 437, 529-533, 2005.

557

558 Cleverly J, Boulain N, Villalobos-Vega R, Grant N, Faux R, Wood C, Cook PG, Yu Q, Leigh A, Eamus D. 2013.
559 Dynamics of component carbon fluxes in a semi-arid Acacia woodland, central Australia. *Journal of Geophysical*
560 *Research-Biogeosciences* 118:1168–1185. doi: 10.1002/jgrg.20101.

561

562 Cleverly, J, Eamus, D, Luo, Q, Restrepo Coupe, N, Kljun, N, Ma, X, Ewenz, C, Li, L, Yu, Q, and Huete, A: The
563 importance of interacting climate modes on Australia's contribution to global carbon cycle extremes, *Scientific Reports*, 6,
564 23113, doi: 10.1038/srep23113, 2016a.

565

566 Cleverly, J, Eamus, D, Van Gorsel, E, Chen, C, Rumman, R, Luo, Q, Restrepo Coupe, N, Li, L, Kljun, N, Faux, R, Yu, Q,
567 and Huete, A: Productivity and evapotranspiration of two contrasting semiarid ecosystems following the 2011 global
568 carbon land sink anomaly, *Agric. For. Meteor.*, 220, 151-159, doi: 10.1016/j.agrformet.2016.01.086, 2016b.

569

570 Cowan IR, Farquhar GD. 1977. Stomatal function in relation to leaf metabolism and environment. Pages 471–505 in
571 Jennings DH, editor. *Integration of Activity in the Higher Plant*. Cambridge University Press, Cambridge.

572

573 CSIRO and Bureau of Meteorology: State of the Climate 2014. Retrieved from [www.bom.gov.au/state-of-the-](http://www.bom.gov.au/state-of-the-climate?documents/state-of-the-climate-2014_low-res.pdf?ref=button)
574 [climate?documents/state-of-the-climate-2014_low-res.pdf?ref=button](http://www.bom.gov.au/state-of-the-climate?documents/state-of-the-climate-2014_low-res.pdf?ref=button), 2014.

575

576 Dai, A.: Increasing drought under global warming in observations and models, *Nature Clim. Change*, 3, 52-58, 2013.

577

578 Dole, R., Hoerling, M., Perlwitz, J., Eischeid, J., Pegion, P., Zhang, T., Quan, X.W., Xu, T. and Murray, D.: Was there a
579 basis for anticipating the 2010 Russian heat wave? *Geophys Res Lett* 38, doi: 10.1029/2010GL046582, 2011.

580

581 Donohue, R. J., Roderick, M. L., McVicar, T. R. and Farquhar, G. D.: Impact of CO₂ fertilization on maximum foliage
582 cover across the globe's warm, arid environments. *Geophys Res Lett*, 40, 3031–3035, 2013.

583

584 Eamus, D., Boulain, N., Cleverly, J. and Breshears, D.D.: Global change-type drought-induced tree mortality: vapor
585 pressure deficit is more important than temperature per se in causing decline in tree health. *Ecology and Evolution*, doi:
586 10.1002/ece3.664. 2013

587

588 Evans, B., Stone, C. and Barber, B.: Linking a decade of forest declines in southwest, Western Australia to bioclimatic
589 change, *Australian Forestry*, 76, 164-172, 2013.

590

591 Evans, B. and Lyons, T.: Bioclimatic Extremes Drive Forest Mortality in Southwest, Western Australia, *Climate*, 1, 36,
592 2013.

593

594 Fischer, E. M., Seneviratne, S. I., Vidale, P. L., Lüthi, D., and Schär, C.: Soil Moisture–Atmosphere Interactions during
595 the 2003 European Summer Heat Wave, *J. Clim.*, 20, 5081-5099, 2007.

596

597 Frank, D., Reichstein, M., Bahn, M., Thonicke, K., Frank, D., Mahecha, M.D., Smith, P., Velde, M., Vicca, S., Babst, F.,
598 Beer, C., Buchmann, N., Canadell, J.G., Ciais, P., Cramer, W., Ibrom, A., Miglietta, F., Poulter, B., Rammig, A.,
599 Seneviratne, S.I. Walz, A., Wattenbach, M., Zawala, M.A., Zscheischler, J.: Effects of climate extremes on the terrestrial
600 carbon cycle: concepts, processes and potential future impacts. *Glob Change Biol*, 21, 2861-2880, doi:
601 10.1111/gcb.12916, 2015.

602

603 Granier, A., Bréda, N., Biron, P. and Villette, S.: A lumped water balance model to evaluate duration and intensity of
604 drought constraints in forest stands. *Ecol Model*, 116, 269-283, 1999.

605

606 Guerlet, S., Basu, S., Butz, A., Krol, M., Hahne, P., Houweling, S., Hasekamp, O.P. and Aben, I.: Reduced carbon uptake
607 during the 2010 Northern Hemisphere summer from GOSAT. *Geophys Res Lett*, DOI: 10.1002/grl.50402, 2013.

608 Hanson, C.E., Palutikof, J.P., Dlugolecki, A., Giannakopoulos, C.: Bridging the gap between science and the stakeholder:
609 the case of climate change research. *Climate Res*, 31, doi:10.3354/r031121. 2006.

610

611 Hansen, J., Sato, M., and Ruedy, R.: Perception of climate change, *Proc. Natl. Acad. Sci. U. S. A.*, 109, E2415-E2423,
612 doi: 10.1073/pnas.1205276109, 2012.

613

614 Hanson, C.E., Palutikof, J.P., Dlugolecki, A. and Giannakopoulos, C.: Bridging the gap between science and the
615 stakeholder: the case of climate change research. *Clim. Res.*, 31, 121–133, 2006.

616

617 Haverd, V. and Cuntz, M.: Soil–Litter–Iso: A one-dimensional model for coupled transport of heat, water and stable
618 isotopes in soil with a litter layer and root extraction, *Journal of Hydrology*, 388, 438-455, 2010.

619

620 Haverd, V., Raupach, M. R., Briggs, P. R., Canadell, J. G., Davis, S. J., Law, R. M., Meyer, C. P., Peters, G. P., Pickett-
621 Heaps, C., and Sherman, B.: The Australian terrestrial carbon budget, *Biogeosciences*, 10, 851-869, 2013a.

622

623 Haverd, V., Raupach, M.R., Briggs, P.R., Canadell, J.G., Isaac, P., Pickett-Heaps, C., Roxburgh, S.H., van Gorsel, E.,
624 Viscarra Rossel, R.A. and Wang, Z.: Multiple observation types reduce uncertainty in Australia's terrestrial carbon and
625 water cycles. *Biogeosciences*, 10, 3, 2011-2040, 2013b.

626

627 Haverd, V, Smith, B, and Trudinger, C: Process contributions of Australian ecosystems to interannual variations in the
628 carbon cycle, *Environ. Res. Lett.*, 11, 7, doi: 10.1088/1748-9326/11/5/054013, 2016.

629

630 Hsu, K., Gupta, H.V., Gao, X., Sorooshian S., and Imam, B.: Self-Organizing Linear Output (SOLO): An artificial neural
631 network suitable for hydrological modeling and analysis. *Water Resour Res*, 38, 1302, doi: 10.1029/2001WR000795,
632 2002.

633

634 Hughes, L.: Climate change and Australia: Trends, projections and impacts, *Austral Ecol*, 28, 423–443, 2003.

635

636 IPCC: Climate Change 2013: The Physical Science Basis. Contribution of Working Group I to the Fifth Assessment
637 Report of the Intergovernmental Panel on Climate Change [Stocker, T.F., D. Qin, G.-K. Plattner, M. Tignor, S.K. Allen, J.
638 Boschung, A. Nauels, Y. Xia, V. Bex and P.M. Midgley (eds.)], Cambridge University Press, Cambridge, UK and New
639 York, USA, 2013.

640
641 Isaac, P., Cleverly, J., Beringer, J., and McHugh, I.: The OzFlux network data path: from collection to curation,
642 Biogeosciences, this issue, 2016.
643
644 Karoly, D., England, M. and Stiffen W.: Off the charts: Extreme Australian summer heat. Report by the Climate
645 Commission, retrieved from <http://climatecommission.angrygoats.net/report/off-charts-extreme-january-heat-2013/>, 2013.
646
647 Keenan, T. F., Hollinger, D.Y., Bohrer, G., Dragoni, D., Munger, J.W., Schmid, H.P. and Richardson A.D.: Increase in
648 forest water-use efficiency as atmospheric carbon dioxide concentrations rise. *Nature* 499, 324–7, 2013.
649
650 King A.D., Karoly, D.J., Donat, M.G. and Alexander, L.V.: Climate change turns Australia’s 2013 Big Dry into a year of
651 record-breaking heat. *B Am Meteorol Soc.*, 95, 41-45, 2014.
652
653 Kljun, N., Black, T.A., Griffis, T.J., Barr, A.G., Gaumont-Guay, D., Morgenstern, K., McCaughey, J.H., Nesic, Z.:
654 Response of Net Ecosystem Productivity of Three Boreal Forest Stands to Drought. *Ecosystems* 10, 1039-1055. doi:
655 10.1007/s10021-007-9088-x, 2007.
656
657 Lee, X., Massman, W. and Law, B.E.: Handbook of micrometeorology. A guide for surface flux measurements and
658 analysis. Kluwer Academic Press, Dordrecht, 250p., 2004.
659
660 Leuning R., Cleugh H.A., Zegelin S.J. and Hughes D.: Carbon and water fluxes over a temperate Eucalyptus forest and a
661 tropical wet/dry savanna in Australia: measurements and comparison with MODIS remote sensing estimates. *Agric For*
662 *Meteorol*, 129, *Agric For Meteorol*, doi: 10.1016/j.agrformet.2004.12.004, 2005.
663
664 Leuning, R., Zegelin, S.J., Jones, K., Keith, H. and Hughes, D.: Measurement of horizontal and vertical advection of CO₂
665 within a forest canopy, *Agric For Meteorol*, 148, doi: 10.1016/j.agrformet.2008.06.006, 2008.
666
667 Lewis, S. C. and King, A. D.: Dramatically increased rate of observed hot record breaking in recent Australian
668 temperatures, *Geophys Res Lett*, 42, 7776-7784, 2015.
669
670 Matusick, G., Ruthrof, K., Brouwers, N., Dell, B. and Hardy, G. J.: Sudden forest canopy collapse corresponding with
671 extreme drought and heat in a mediterranean-type eucalypt forest in southwestern Australia. *Eur J Forest Res*, 132, 497–
672 510, 2013.
673

674 McDowell, N., Pockman, W.T., Allen, C.D., Breshears, D.D., Cobb, N., Kolb, T., Plaut, J., Sperry, J., West, A., Williams,
675 D.G. and Yezzer, E.A.: Mechanisms of plant survival and mortality during drought: why do some plants survive while
676 others succumb to drought?. *New phytologist*, doi: 10.1111/j.1469-8137.2008.02436.x., 2008.
677
678 Meyer, W.S., Kondrlova, E. and Koerber, G.R.: Evaporation of perennial semi-arid woodland in southeastern Australia is
679 adapted for irregular but common dry periods. *Hydrol Process*, doi: 10.1002/hyp.10467, 2015.
680
681 Mitchell, P. J., O’Grady, A. P., Hayes, K. R. and Pinkard, E. A.: Exposure of trees to drought-induced die-off is defined
682 by a common climatic threshold across different vegetation types., *Ecol Evol*, 4(7), 1088–101, doi: 10.1002/ece3.1008,
683 2014.
684
685 Oliver, J.E.: Bowen Ratio, *Climatology*, Part of the series *Encyclopedia of Earth Science*, doi: 10.1007/0-387-30749-
686 4_30, 1987.
687
688 Perkins, SE, Argueso, D, and White, CJ: Relationships between climate variability, soil moisture, and Australian
689 heatwaves, *J. Geophys. Res.-Atmos.*, 120, 8144-8164, doi: 10.1002/2015jd023592, 2015.
690
691 Pfautsch, S. and Adams, M. A.: Water flux of Eucalyptus regnans: Defying summer drought and a record heat wave in
692 2009. *Oecologia*, 172, 317–326. doi: 10.1007/s00442-012-2494-6, 2013.
693
694 Poulter, B., Frank, D., Ciais, P., Myneni, R. B., Andela, N., Bi, J., Broquet, G., Canadell, J. G., Chevallier, F., Liu, Y. Y.,
695 Running, S. W., Sitch, S., and van der Werf, G. R.: Contribution of semi-arid ecosystems to interannual variability of the
696 global carbon cycle, *Nature*, 509, 600-603, 2014.
697
698 Raupach, M.R., Briggs, P.R., Haverd, V., King, E.A., Paget, M. and Trudinger, C.M.: Australian Water Availability
699 Project (AWAP): CSIRO Marine and Atmospheric Research Component: Final Report for Phase 3, CACWR technical
700 report, http://www.csiro.au/awap/doc/CTR_013_online_FINAL.pdf, 2009.
701
702 Reichstein, M., Ciais, P., Papale, D., Valentini, R., Running, S., Viovy, N., Cramer, W., Granier, A., Ogee, J., Allard, V.,
703 Aubinet, M., Bernhofer, Chr., Buchmann, N., Carrara, A., Grunwald, T., Heimann, M., Heinesch, B., Knohl, A., Kutsch,
704 W., Loustau, D., Manca, G., Matteucci, G., Miglietta, G., Ourcival, J.M., Pilegaard, K., Pumpanen, J., Rambal, S.,
705 Schapphoff, S., Seufert, G., Soussana, J.F., Sanz, M.J., Vesala, T. and Zhao, M.: Reduction of ecosystem productivity and
706 respiration during the European summer 2003 climate anomaly: a joint flux tower, remote sensing and modelling
707 analysis. *Glob Change Biol*, 13(3), doi: 10.1111/j.1365-2486.2006.01224.x, 2007.

708

709 Reichstein, M., Bahn, M., Ciais, P., Frank, D., Mahecha, M. D., Seneviratne, S. I., Zscheischler, J., Beer, C., Buchmann,
710 N., Frank, D. C., Papale, D., Rammig, A., Smith, P., Thonicke, K., van der Velde, M., Vicca, S., Walz, A., and
711 Wattenbach, M.: Climate extremes and the carbon cycle, *Nature*, 500, 287-295, 2013.

712

713 Richardson, A.D., Braswell, B.H., Hollinger, D.Y., Burman, P., Davidson, E.A., Evans, R.S., Flanagan, L.B., Munger,
714 J.W., Savage, K., Urbanski, S.P. and Wofsy, S.C., 2006. Comparing simple respiration models for eddy flux and dynamic
715 chamber data. *Agr Forest Meteorol*, 141(2), doi: 10.1016/j.agrformet.2006.10.010, 2006.

716

717 Schär, C., Vidale, P. L., Luthi, D., Frei, C., Haberli, C., Liniger, M. A., and Appenzeller, C.: The role of increasing
718 temperature variability in European summer heatwaves, *Nature*, 427, 332-336, 2004.

719

720 Schlesinger, W. H., Dietze, M. C., Jackson, R. B., Phillips, R. P., Rhoades, C. C., Rustad, L. E., and Vose, J. M.: Forest
721 biogeochemistry in response to drought, *Glob. Change Biol.*, 22, 2318-2328, 2016.

722

723 Schotanus, P., Nieuwstadt F. T. M., and de Bruin H. A. R.: Temperature measurement with a sonic anemometer and its
724 application to heat and moisture fluxes, *Bound Lay Meteor*, 26, 81–93, 1983.

725

726 Seneviratne, S. I., Corti, T., Davin, E. L., Hirschi, M., Jaeger, E. B., Lehner, I., Orlowsky, B., and Teuling, A. J.:
727 Investigating soil moisture-climate interactions in a changing climate: A review, *Earth-Sci. Rev.*, 99, 125-161, 2010.

728

729 Sheffield, J., Wood, E. F., and Roderick, M. L.: Little change in global drought over the past 60 years, *Nature*, 491, 435-
730 438, 2012.

731

732 Steffen, W.: Quantifying the impact of climate change on extreme heat in Australia. Report by the Climate Council of
733 Australia, retrieved from <http://www.climatecouncil.org.au/uploads/00ca18a19ff194252940f7e3c58da254.pdf>, 2015.

734

735 Steffen, W., Hughes, L. and Perkins, S.: Heatwaves: hotter, longer, more often. Report by the Climate Council of Australia,
736 retrieved from <http://www.climatecouncil.org.au/uploads/9901f6614a2cac7b2b888f55b4dff9cc.pdf>, 2014.

737

738 Sulman, B. N., Roman, D. T., Yi, K., Wang, L., Phillips, R. P., and Novick, K. A.: High atmospheric demand for water
739 can limit forest carbon uptake and transpiration as severely as dry soil, *Geophys. Res. Lett.*, doi: 10.1002/2016GL069416,
740 2016. n/a-n/a, 2016.

741

742 Sun, Q., Meyer, W.S., Koerber, G.R. and Marschner, P.: Response of respiration and nutrient availability to drying and
743 rewetting in soil from a semi-arid woodland depends on vegetation patch and a recent wildfire, *Biogeosciences*, doi:
744 10.5194/bg-12-5093-2015, 2015.

745

746 Tanner, C. B. and Thurtell, G. W.: Anemoclinometer measurements of Reynolds stress and heat transport in the
747 atmospheric surface layer, Research and Development Tech. Report ECOM 66-G22-F to the US Army Electronics
748 Command, Dept. Soil Science, Univ. of Wisconsin, Madison, WI, 1969.

749

750 Teuling, A.J., Seneviratne, S.I., Stöckli, R., Reichstein, M., Moors, E., Ciais, P., Luyssaert, S., van den Hurk, B.,
751 Ammann, C., Bernhofer, C. and Dellwik, E., Gianelle, D., Gielen, B., Grünwald, Th., Klumpp, K., Montagnani, L.,
752 Moureaux, Ch., Sottocornola, M. and Wohlfahrt, G.: Contrasting response of European forest and grassland energy
753 exchange to heatwaves. *Nature Geoscience*, 3, doi: 10.1038/NGEO950, 2010.

754

755 Trenberth, K. E., Dai, A., van der Schrier, G., Jones, P. D., Barichivich, J., Briffa, K. R., and Sheffield, J.: Global
756 warming and changes in drought, *Nature Clim. Change*, 4, 17-22, 2014.

757

758 Tuzet, A., Perrier, A. and Leuning, R.: A coupled model of stomatal conductance, photosynthesis and transpiration. *Plant,*
759 *Cell and Environment*, 1097–1116, 2003.

760

761 Ukkola, A. M. Prentice, I.C., Keenan, T.F., van Dijk, A.I., Viney, N.R., Myneni, R.B. and Bi, J.: Reduced streamflow in
762 water-stressed climates consistent with CO₂ effects on vegetation. *Nat Clim Chang* 6, 75–78, 2015.

763

764 van der Molen, M. K., Dolman, A. J., Ciais, P., Eglin, T., Gobron, N., Law, B. E., Meir, P., Peters, W., Phillips, O. L.,
765 Reichstein, M., Chen, T., Dekker, S. C., Doubkova, M., Friedl, M. A., Jung, M., van den Hurk, B. J. J. M., de Jeu, R. A.
766 M., Kruijt, B., Ohta, T., Rebel, K. T., Plummer, S., Seneviratne, S. I., Sitch, S., Teuling, A. J., van der Werf, G. R., and
767 Wang, G.: Drought and ecosystem carbon cycling, *Agric. For. Meteorol.*, 151, 765-773, 2011.

768

769 van Gorsel, E., Leuning, R., Cleugh, H.A., Keith, H. and Suni, T., 2007: Nocturnal carbon efflux: Reconciliation of eddy
770 covariance and chamber measurements using an alternative to the u*-threshold filtering technique, *Tellus B*, 59, doi:
771 10.1111/j.1600-0889.2007.00252.x, 2007.

772

773 van Gorsel, E., Delpierre, N., Leuning, R., Black, A., Munger, J.W., Wofsy, S., Aubinet, M., Feigenwinter, Ch.,
774 Beringer, J., Bonal, D., Chen, B., Chen, J., Clement, R., Davis, K.J., Desai, A.R., Dragoni, D., Etzold, S., Grünwald, T.,
775 Gu, L., Heinesch, B., Hutyrá, L.R., Jans, W.W.P., Kutsch, W., Law, B.E., Leclerc, M.Y., Mammarella, I., Montagnani, L.,

776 Noormets, A., Rebmann, C. and Wharton S.: Estimating nocturnal ecosystem respiration from the vertical turbulent flux
777 and change in storage of CO₂, *Agric For Meteorol*, 149, doi: 10.1016/j.agrformet.2009.06.020, 2009.
778

779 van Gorsel, E., Berni, J.A.J., Briggs, P., Cabello-Leblic, A., Chasmer, L., Cleugh, H.A., Hacker, J., Hantson, S., Haverd,
780 V., Hughes, D. and Hopkinson, C., Keith, H., Kljun, N., Leuning, R., Yebra, M. and Zegelin, S.: Primary and secondary
781 effects of climate variability on net ecosystem carbon exchange in an evergreen Eucalyptus forest, *Agric For Meteorol*,
782 182, doi: 10.1016/j.agrformet.2013.04.027, 2013.
783

784 van Heerwaarden, C. C. and Teuling, A. J.: Disentangling the response of forest and grassland energy exchange to
785 heatwaves under idealized land–atmosphere coupling, *Biogeosciences*, 11, 6159-6171, 2014.
786

787 Wang, Y. P., Law, R. M., and Pak, B.: A global model of carbon, nitrogen and phosphorus cycles for the terrestrial
788 biosphere, *Biogeosciences*, 7, 2261-2282, 2010.
789

790 Wang, Y.P., Kowalczyk, E., Leuning, R., Abramowitz, G., Raupach, M.R., Pak, B., van Gorsel, E., Luhar, A.: Diagnosing
791 errors in a land surface model (CABLE) in the time and frequency domains, *J Geophys Res*, 116, doi:
792 10.1029/2010JG001385, 2011.
793

794 Webb, E., Pearman, G. and Leuning R.: Correction of flux measurements for density effects due to heat and water vapor
795 transfer, *Q J Roy Meteor Soc*, 106, 85–100, 1980.
796

797 Wesely, M., 1970: Eddy correlation measurements in the atmospheric surface layer over agricultural crops. Ph. D.
798 Dissertation, 102pp., 1970.
799

800 Whan, K., Zscheischler, J., Orth, R., Shongwe, M., Rahimi, M., Asare, E.O. and Seneviratne, S.I.: Impact of soil moisture
801 on extreme maximum temperatures in Europe. *Weather and Climate Extremes*, 9, 57-67, 2015
802

803 Wolf, S., Eugster, W., Ammann, C., Häni, M., Zielis, S., Hiller, R., Stieger, J., Imer, D., Merbold, L., and Buchmann, N.:
804 Contrasting response of grassland versus forest carbon and water fluxes to spring drought in Switzerland, *Environ. Res.*
805 *Lett.*, 8, 035007, 2013.
806

807 Wolf, S., Keenan, T. F., Fisher, J. B., Baldocchi, D. D., Desai, A. R., Richardson, A. D., Scott, R. L., Law, B. E., Litvak,
808 M. E., Brunsell, N. A., Peters, W., and van der Laan-Luijkx, I. T.: Warm spring reduced carbon cycle impact of the 2012

809 US summer drought, Proceedings of the National Academy of Sciences, 113, 5880-5885, 2016.
810
811 Wolf S, Yin D, Roderick ML: Using radiative signature to diagnose the cause of warming associated with the Californian
812 Drought. Journal of Geophysical Research - Atmospheres, in review
813
814 Yuan, W., Cai, W., Chen, Y., Liu, S., Dong, W., Zhang, H., Yu, G., Chen, Z., He, H., Guo, W., Liu, D., Liu, S., Xiang,
815 W., Xie, Z., Zhao, Z. and Zhou, G.: Severe summer heatwave and drought strongly reduced carbon uptake in Southern
816 China. Scientific Reports - Nature, 18813. doi: 10.1038/srep18813, 2015.
817
818 Zhang, Y, Xiao, XM, Zhou, S, Ciais, P, McCarthy, H, and Luo, YQ: Canopy and physiological controls of GPP during
819 drought and heat wave, Geophys. Res. Lett., 43, 3325-3333, doi: 10.1002/2016gl068501, 2016.
820
821 Zhao, M. and Running, S. W.: Drought-Induced Reduction in Global Terrestrial Net Primary Production from 2000
822 Through 2009. Science, 329(5994), 940–943. doi: 10.1126/science.1192666, 2010.
823
824 Zhu, Z., Bi, J., Pan, Y., Ganguly, S., Anav, A., Xu, L., Samanta, A., Piao, S., Nemani, R.R., Myneni, R.B.: Global Data
825 Sets of Vegetation Leaf Area Index (LAI)3g and Fraction of Photosynthetically Active Radiation (FPAR)3g Derived from
826 Global Inventory Modeling and Mapping Studies (GIMMS) Normalized Difference Vegetation Index (NDVI3g) for the
827 Period 1981 to 2011, Remote Sens., 5, doi: 10.3390/rs5020927, 2013.
828
829 Zimmermann, N. E., N. G. Yoccoz, T. C. Edwards, E. S. Meier, W. Thuiller, A. Guisan, et al. 2009. Climatic extremes
830 improve predictions of spatial patterns of tree species. Proc Natl Acad Sci, 106, 19723–19728, 2009.
831
832 Zscheischler, J., Orth, R. and Seneviratne, S.I.: A submonthly database for detecting changes in vegetation-atmosphere
833 coupling. Geophys Res Lett, doi: 10.1002/2015gl066563, 2015.

834

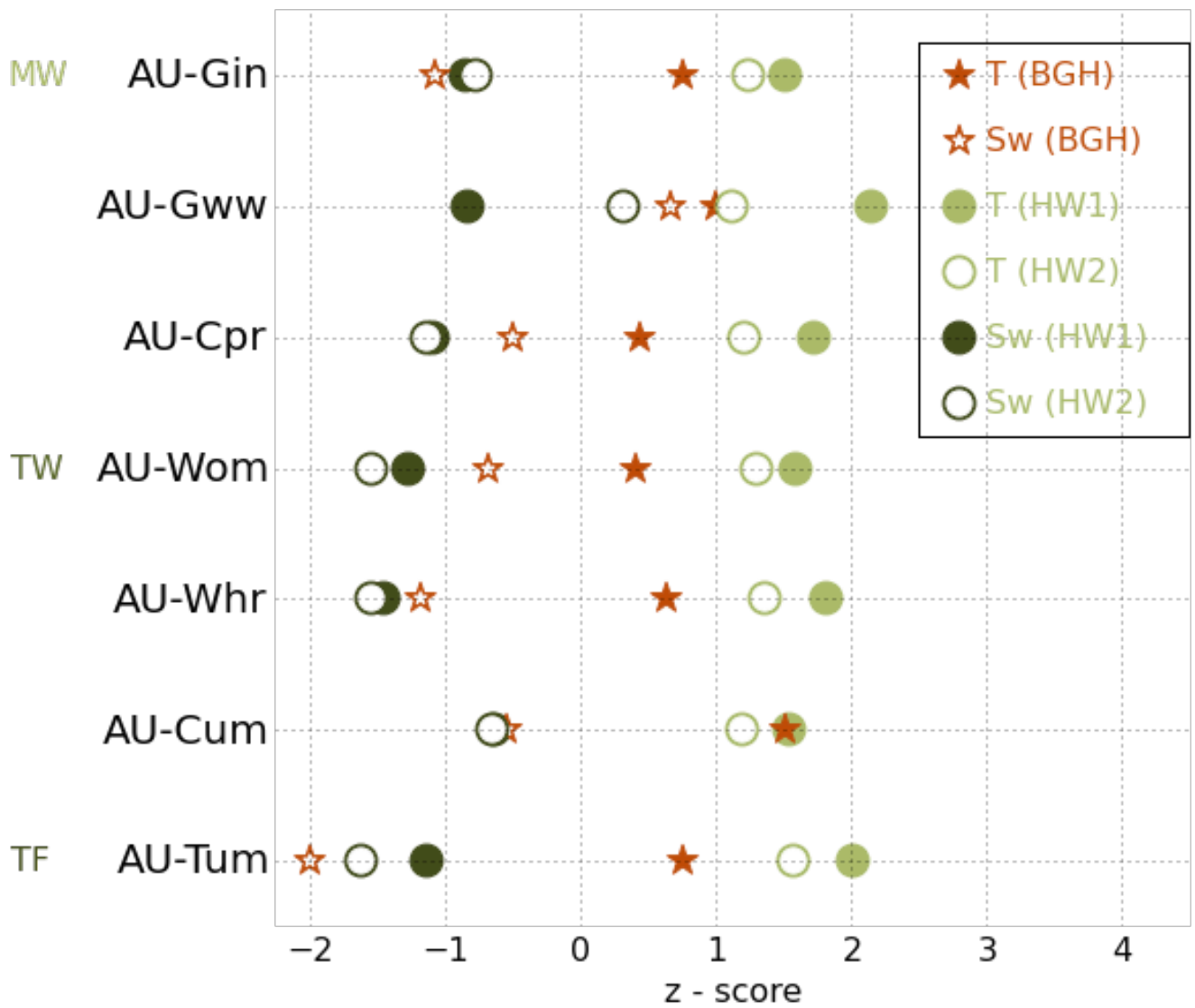
835 **Figures**



836

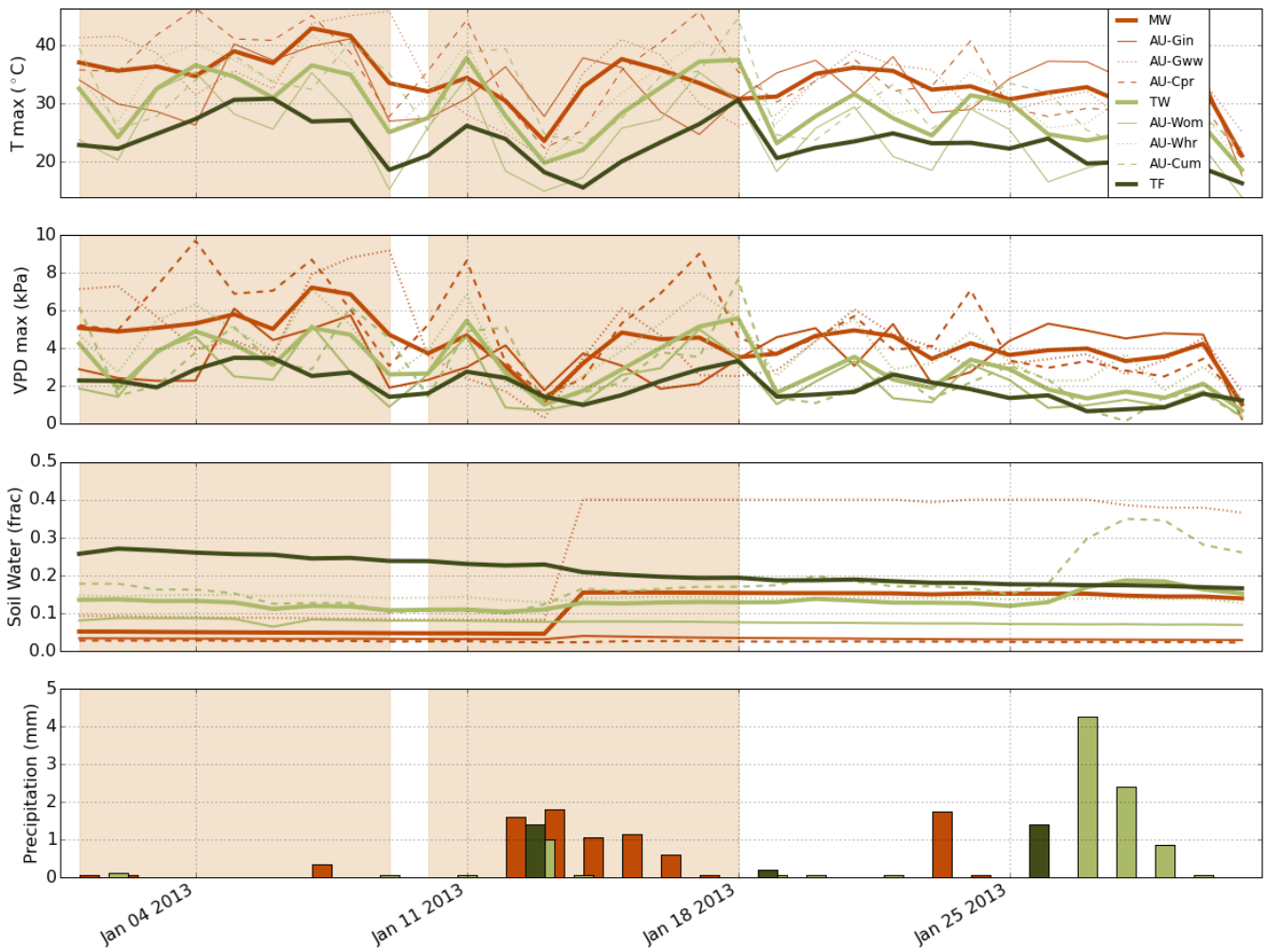
837 Figure 1. Map indicating the locations of the OzFlux sites used in this study. The sites are grouped into three distinct
838 climate and ecosystem types, indicated by red dots for Mediterranean woodlands (MW), light green dots for temperate
839 woodlands (TW) and a dark green dot for the temperate forest (TF)

840

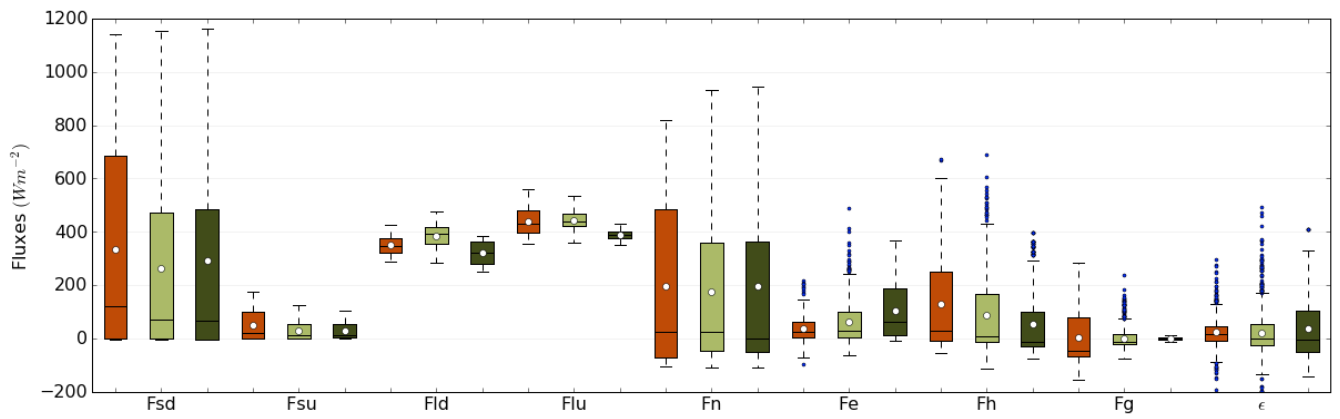


841

842 Figure 2. z-scores for temperature and soil water across flux tower sites. Solid red stars denote temperature and unfilled
 843 red stars denote soil water scores during the background period (BGH) compared to the climatological background BGC.
 844 Scores for temperature (T) and soil water (Sw) for HW1 and HW2 compared to the same time periods in the years 1982-
 845 2013 are shown for HW1 (1/1/2013–9/1/2013) by filled dots and for HW2 (10/1/2013–18/1/2013) by unfilled dots.



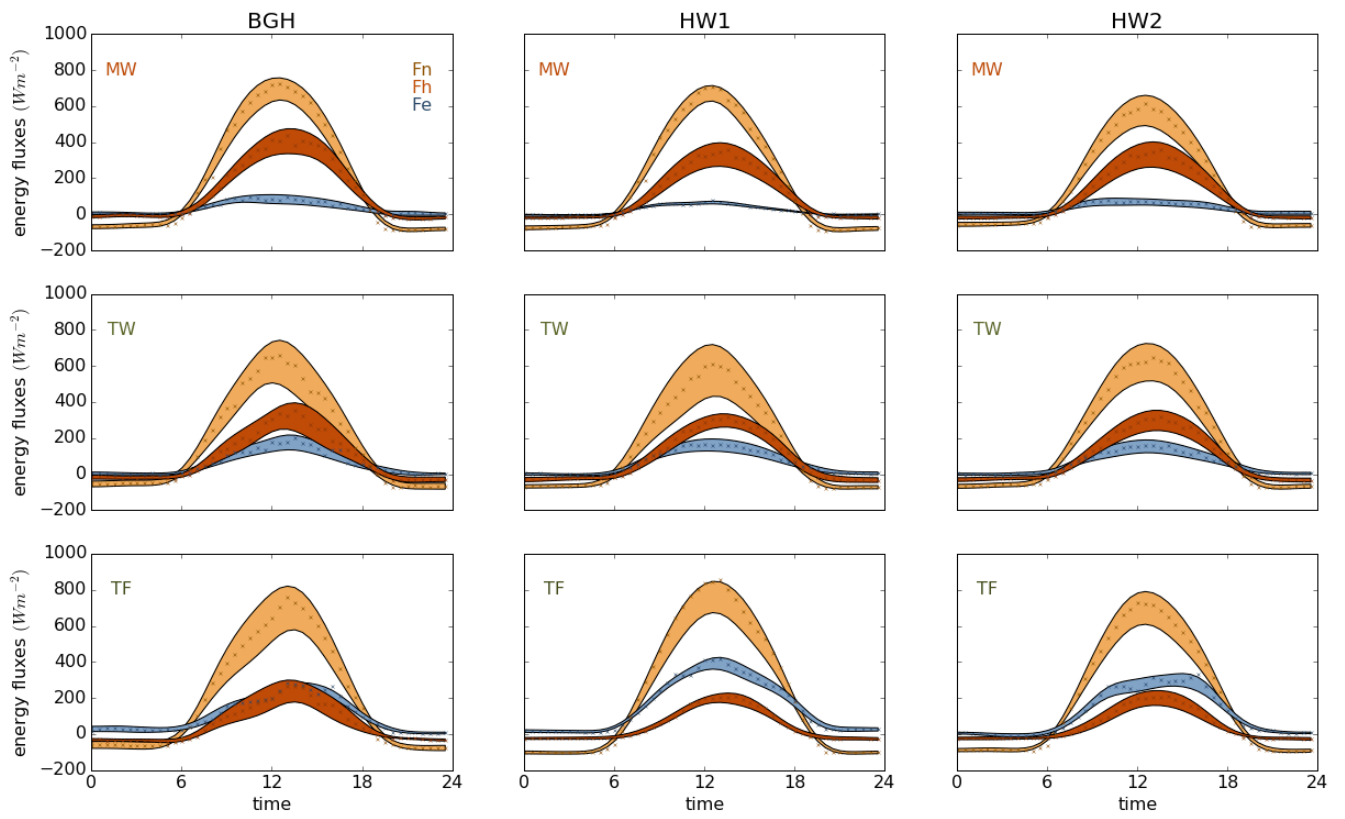
846
 847 Figure 3. Time series of daily maximum temperature (T max, top panel), daily maximum vapour pressure deficit (VPD
 848 max), soil water content and precipitation. The legend is given in the top panel. Precipitation (P) is given as the average of
 849 the daily accumulated precipitation of the sites and displayed for each biome. Shaded areas in the background indicate the
 850 time periods HW1 and HW2.



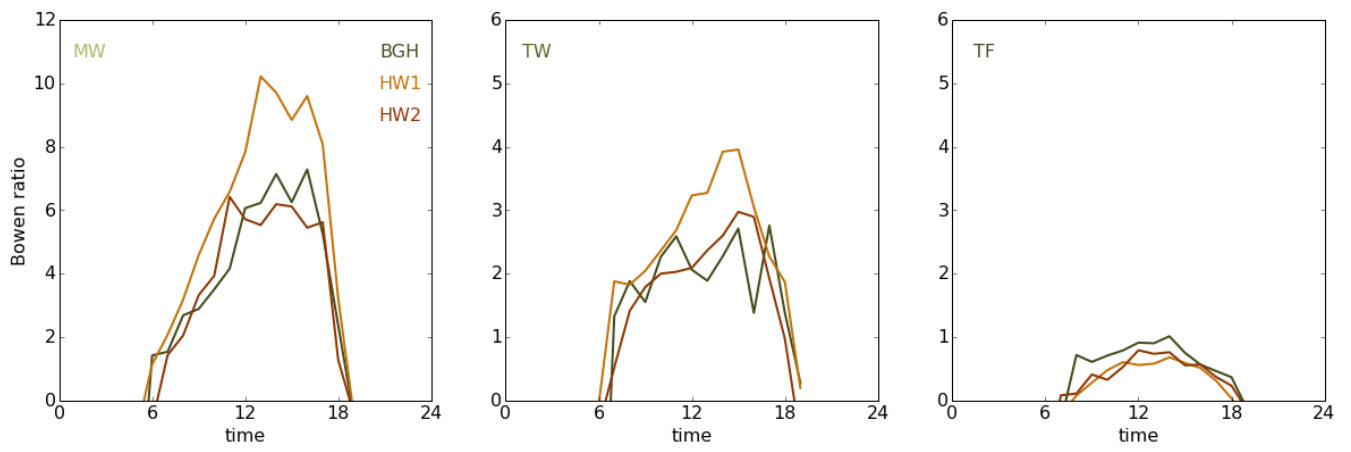
851

852 Figure 4. Box plot of energy fluxes for Mediterranean woodlands (MW, red), temperate woodlands (TW, light green) and
 853 temperate forests (TF, dark green). Energy fluxes are incoming shortwave radiation (Fsd), reflected shortwave radiation
 854 (Fsu), downward longwave radiation (Fld), emitted longwave radiation (Flu), net radiation (Fn), latent heat flux (Fe),
 855 sensible heat flux (Fh), ground heat flux (Fg) and energy imbalance (ϵ) during the background period BGH (2/1/2014 –
 856 6/1/2014). The box extends from the lower to upper quartile values of the data, with a line at the median. The mean value
 857 is indicated with a dot. The whiskers extend from the box to show the range of the data. Flier points (outliers, blue dots)
 858 are those past the end of the whiskers.

859



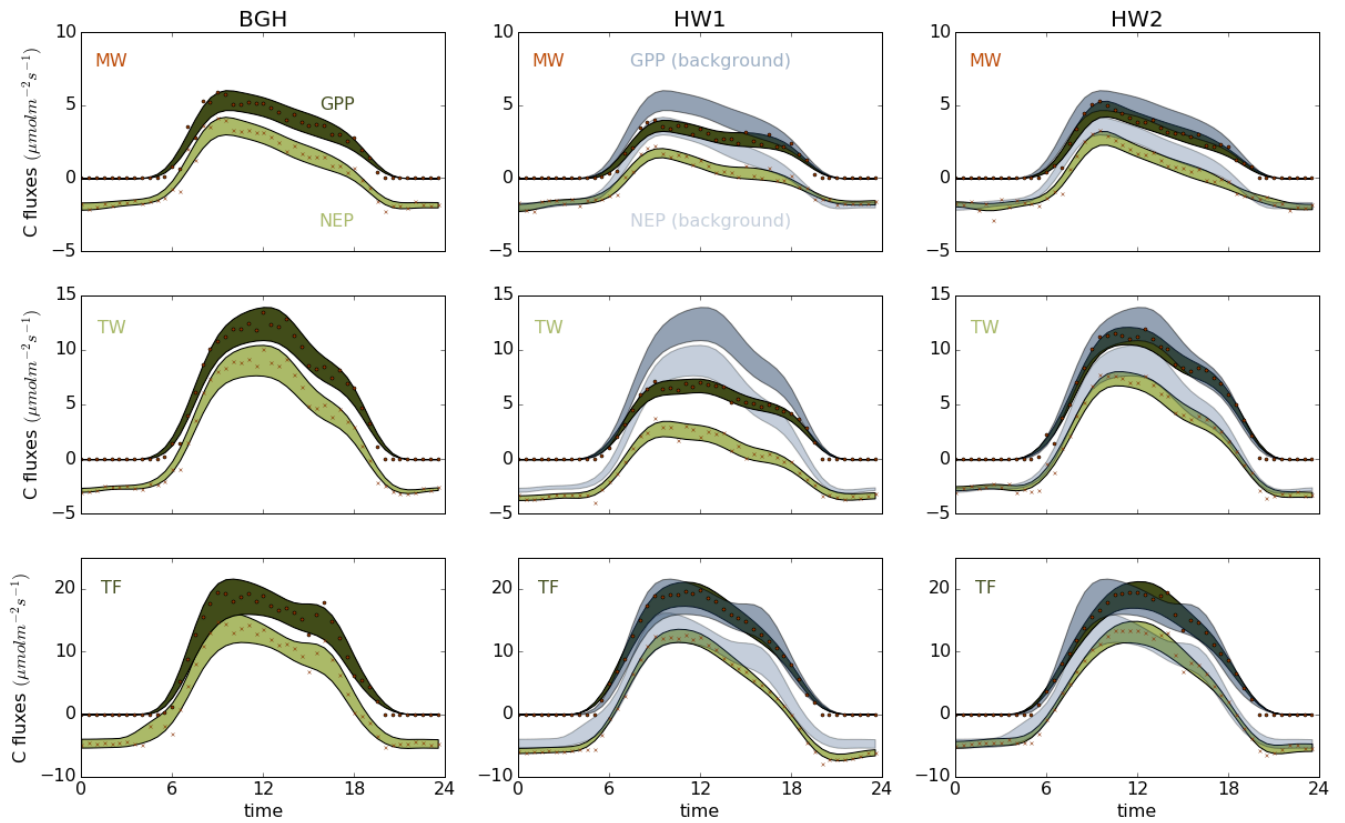
860
 861 Figure 5. Diurnal course of net radiation (Fn, light amber), sensible (Fh, red) and latent (Fe, blue) heat at the
 862 Mediterranean woodlands (MW, top row), the temperate woodlands (TW, middle row) and the temperate forest (TF,
 863 lowest row) for the background period BGH (2/1/2014 – 6/1/2014), and the first and second period of the heat wave
 864 (HW1 (1/1/2013–9/1/2013), HW2 (10/1/2013–18/1/2013)). Filled areas indicate the range of smoothed ± 1 standard
 865 deviation, average mean values are indicated by symbols.
 866
 867



868

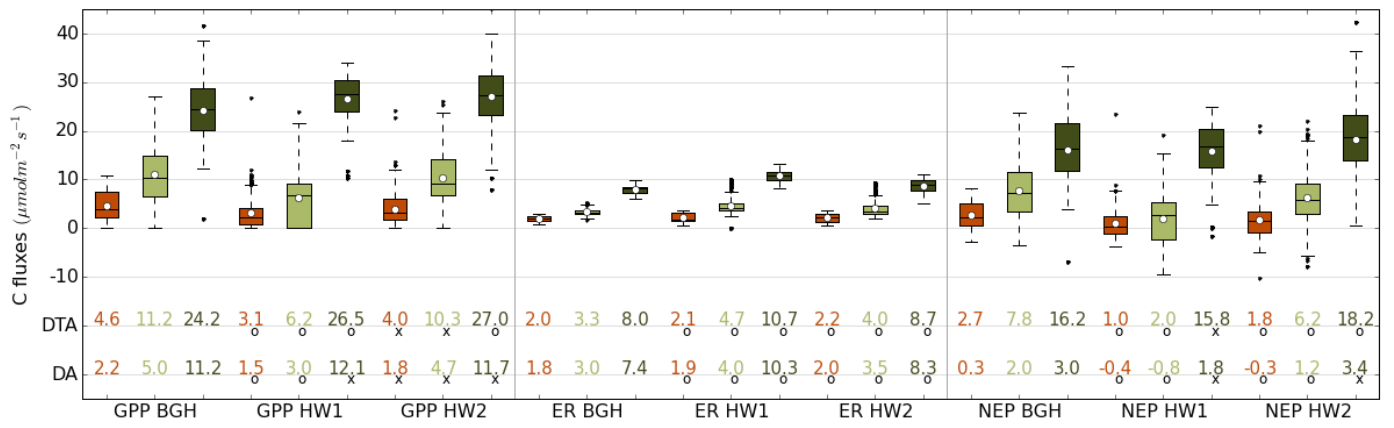
869 Figure 6. Average daytime Bowen ratio measured over Mediterranean woodlands (MW, left panel), the temperate
 870 woodlands (TW, middle panel) and the temperate forest (TF, right panel) for BGH (green line), HW1 (light amber) and
 871 HW2 (dark amber).

872



874

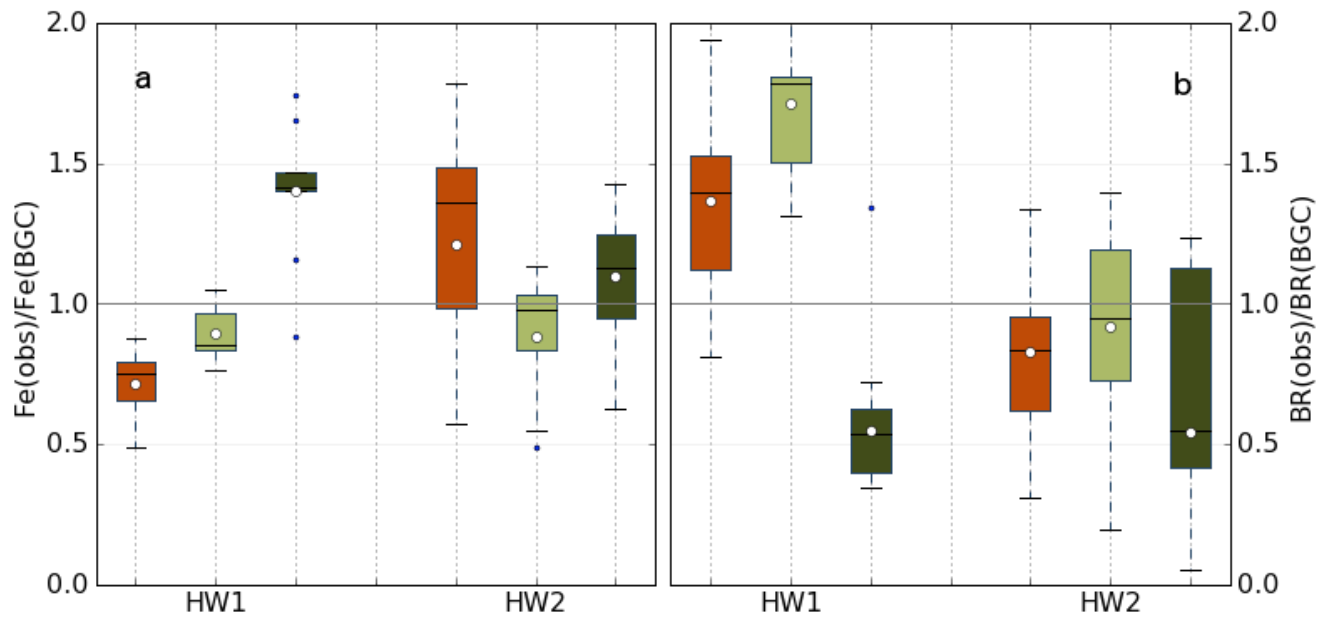
875 Figure 7. Diurnal course of net ecosystem productivity (NEP, light green) and gross primary productivity (GPP, dark
 876 green) at the Mediterranean woodlands (MW, top row), the temperate woodlands (TW, middle row) and the temperate
 877 forest (TF, lowest row) for the background period (BGH), and the first and second period of the heat wave (HW1, HW2).
 878 Filled areas indicate the range of smoothed ± 1 standard deviation values, average mean values are indicated by red
 879 symbols. Background GPP values (dark grey) and NEP values (light grey) are also plotted in HW1 and HW2 to allow for
 880 easier comparison.
 881



883

884 Figure 8. Boxplot of daytime values (9:00-16:00 local standard time) of gross primary productivity (GPP), ecosystem
 885 respiration (ER) and net ecosystem productivity (NEP) for the background period (BGH) and the first and second period
 886 of the heat wave (HW1, HW2). Daytime average values (DTA) are given below boxes and symbols indicate that they are
 887 significantly different from the background period (o) or not (x). Daily averages (DA, 0:00-23:00, local standard time) and
 888 their significance are also given. Colours as in Fig. 1.

889

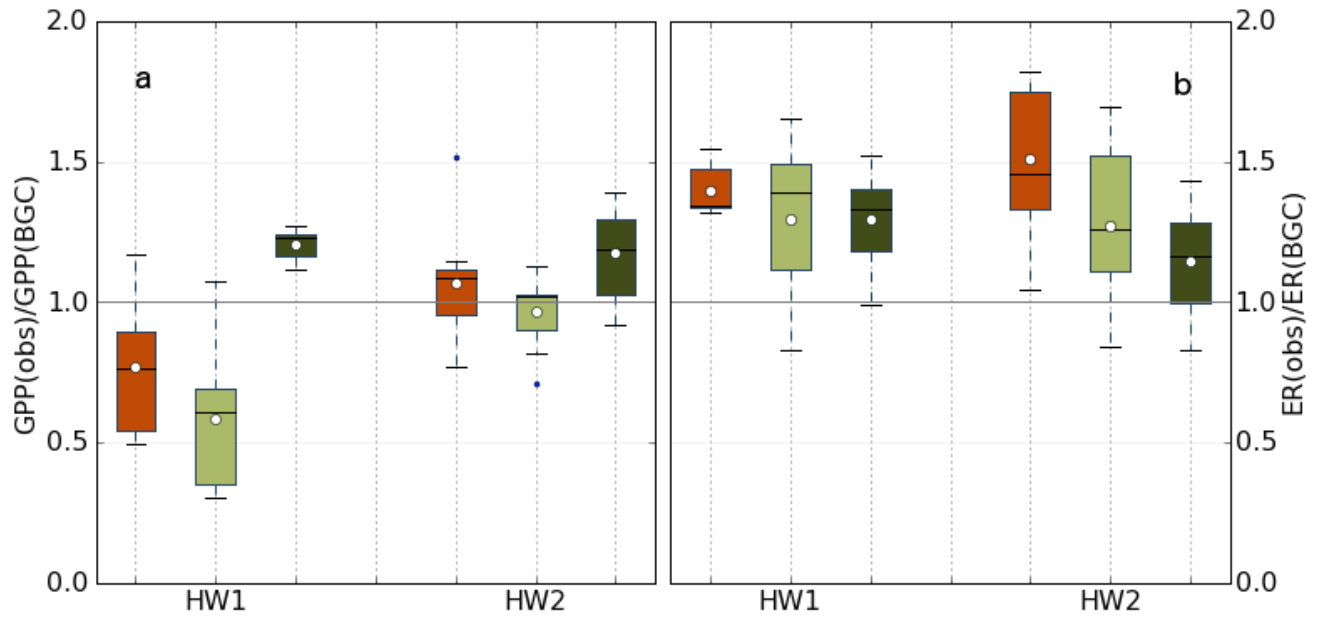


891

892 Figure A1. Left panel: Boxplot of the ratio of observed latent heat ($Fe(obs)$) to the BIOS2 climatology of the latent heat
893 flux ($Fe(BGC)$) during the first and second period of the heat wave (HW1, HW2). Right panel: same as left but for the
894 Bowen ratio. Colours as in Fig. 1.

895

895



897

898 Figure A2. Left panel: Boxplot of the ratio of observed gross primary productivity ($GPP(obs)$) to the climatology of GPP
899 ($GPP(BGC)$) during the first and second period of the heat wave (HW1, HW2). Right panel: same as left but for the ER.

900 Colours as in Fig. 1.

901 **Tables**

902 **Table 1.** List of OzFlux sites used in this study, abbreviations and site information. MW stands for Mediterranean
 903 woodlands, TW for temperate woodlands and TF for temperate forest. MAT and MAP are the mean annual temperature
 904 and precipitation for the years 1982-2013 (BIOS2).

ID	Site Name	Latitude (deg)	Longitude (deg)	Elevation (m)	MAT (°C)	MAP (mm)	LAI Modis (m ² m ⁻²)	Tree Height (m)	Biome
AU-Gin	Gingin	-31.375	115.714	51	18.4	681	0.9	7	MW
AU-Gww	Great Western Woodlands	-30.192	120.654	450	18.7	396	0.4	25	MW
AU-Cpr	Calperum	-34.004	140.588	67	17.0	265	0.5	4	MW
AU-Wom	Wombat	-37.422	144.094	702	11.4	936	4.1	25	TW
AU-Whr	Whroo	-36.673	145.029	155	14.6	533	0.9	30	TW
AU-Cum	Cumberland Plains	-33.613	150.723	33	17.6	818	1.3	23	TW
AU-Tum	Tumbarumba	-35.657	148.152	1260	9.8	1417	4.1	40	TF

905

906

907

908 **Table 2.** Statistics of radiation and energy exchange for the ecosystems Mediterranean Woodlands (MW), Temperate
 909 Woodlands (TW) and Temperate Forests (TF) and the variables flux of shortwave downward radiation (Fsd), shortwave
 910 upward radiation (Fsu), longwave downward radiation (Fld), longwave upward radiation (Flu), net radiation (Fn), latent
 911 heat (Fe), sensible heat (Fh), ground heat (Fg) and the energy imbalance (ϵ). Where values during the two periods of the
 912 heat wave (Δ HW1 and Δ HW2) differ significantly from the background (BGH) ($P < 0.1$) this is indicated by bold fonts.
 913

	MW	TW	TF	MW	TW	TF	MW	TW	TF	MW	TW	TF	MW	TW	TF	MW	TW	TF	MW	TW	TF	MW	TW	TF			
	Fsd			Fsu			Fld			Flu			Fn			Fe			Fh			Fg			ϵ		
BGH	335	264	293	49	30	31	350	383	323	439	444	387	197	175	197	38	63	103	130	90	55	5	1	0	24	21	39
Δ HW1	-10	4	70	-1	0	3	38	9	0	49	33	41	-19	-20	26	-12	2	52	-5	30	-8	6	4	5	-8	-56	-23
Δ HW2	-62	20	16	-10	2	14	36	2	-13	19	16	12	-35	3	-8	-3	-2	14	-29	-4	-8	-5	1	0	1	8	-14

914

915 **Table A1.** Parameters of robust linear model fit between observations and BIOS2 output for all sites, the variables latent
 916 heat flux (Fe), gross primary productivity (GPP), ecosystem respiration (ER) and the time interval 1/1/2013 – 31/12/2013.

variable	ID	coeff	stderr	[95% conf. int.]		RMSE	r ²
Fe							
	AU-Gin	0.9998	5.87e-06	1.000	1.000	27.52	0.44
	AU-Gww	0.9285	0.0032	0.867	0.990	23.13	0.58
	AU-Cpr	0.7464	0.032	0.684	0.809	15.75	0.41
	AU-Wom	1.1253	0.017	1.093	1.158	18.55	0.89
	AU-Whr	0.8917	0.031	0.830	0.953	23.66	0.42
	AU-Cum	1.0385	0.020	0.999	1.078	28.75	0.53
	AU-Tum	0.8121	0.014	0.784	0.840	36.61	0.65
GPP							
	AU-Gin	1.0570	0.035	0.988	1.126	1.91	0.42
	AU-Gww	0.3496	0.031	0.290	0.410	0.95	0.15
	AU-Cpr	0.2806	0.021	0.240	0.321	1.06	0.10
	AU-Wom	1.0176	0.015	0.988	1.047	1.53	0.81
	AU-Whr	1.0194	0.037	0.947	1.092	2.32	0.38
	AU-Cum	1.8764	0.037	1.803	1.949	2.81	0.48
	AU-Tum	0.6667	0.006	0.655	0.679	3.20	0.88
ER							
	AU-Gin	1.1687	0.043	1.084	1.253	2.20	0.13
	AU-Gww	0.4483	0.015	0.420	0.477	0.66	0.31

AU-Cpr	0.3492	0.013	0.324	0.374	0.73	0.01
AU-Wom	1.2682	0.035	1.199	1.337	2.56	0.48
AU-Whr	1.4227	0.039	1.347	1.499	1.87	0.14
AU-Cum	2.0017	0.031	1.941	2.063	2.62	0.66
AU-Tum	0.8770	0.013	0.852	0.902	1.69	0.77

917
918